scientific reports

Check for updates

OPEN

# Mechanical, microstructure, durability, and economic assessment of nano titanium dioxide integrated concrete

Ibadur Rahman[1], Sagar Paruthi[2], Nirendra Dev[3], Mohammed Arif[4], Afzal Husain Khan[5]✉, Mohd Abul Hasan[6], C. Venkata Siva Rama Prasad[7] & Ahmad Alyaseen[8]✉

**Nanotechnology has emerged as a transformative approach to enhancing the concrete properties. This research examines the impact of nano-titanium dioxide (NT) on the concrete properties. NT was incorporated in varying dosages (0.5%, 1%, and 1.5% by weight of the cement) to assess its impact on strength, toughness, and resilience. The results demonstrated a significant enhancement in mechanical properties, with a peak compressive strength of 65.20 ± 1.03 MPa, a split tensile strength of 3.44 ± 0.17 MPa, and a flexural strength of 9.5 ± 0.47 MPa at a 1.5% NT dosage after 28 days of curing. Furthermore, the long-term performance was notable, as the compressive strength further increased to 75.25 ± 1.10 MPa at 180 days, confirming the sustained strength-gain potential of NT-incorporated concrete. Also, durability assessments were conducted under aggressive conditions, including exposure to 4% NaCl, HCl, and $H_2SO_4$ for 90 days. Additional tests, including rapid chloride penetrability test (RCPT), surface resistivity, freeze-thaw resistance, and accelerated carbonation, were conducted to assess long-term durability along with its economic feasibility. The NT-incorporated concrete demonstrated enhanced resistance to chloride ingress, acid attack, and elevated temperatures (200–600 °C), with improved modulus of elasticity and fire resistance. Furthermore, durability assessments revealed a noteworthy contrast, i.e., while resistivity tests classified NT-incorporated concretes as having 'very low' chloride penetrability, RCPT values remained in the 'moderate' category. This divergence underscores the need for multiple durability indices in evaluating nano-concretes. Microstructural analyses using scanning electron microscopy confirmed the densification effect of NT, leading to a refined pore structure and improved bond efficiency within the cementitious matrix. Moreover, economic analysis confirms the economic viability of nano-titanium concrete, demonstrating significant long-term savings through service life extension despite higher initial investment. This research highlights the potential of NT in developing high-performance, durable concrete, reinforcing the importance of nanotechnology in construction industry.**

**Keywords** Durability, Petrographic analysis, Non-destructive tests, Microstructure, Nano titanium dioxide

Titanium dioxide ($TiO_2$) at the nanoscale has gained great research interest due to its unique photocatalytic properties and multifunctional applications. Originally identified by Fujishima and Honda, the Honda-Fujishima effect demonstrated $TiO_2$'s ability to split water into hydrogen and oxygen under UV light exposure, laying the foundation for its widespread application in photocatalysis and environmental remediation. Today, nano-$TiO_2$ (NT) is extensively utilized across various industries, including paints, cosmetics, ceramics, and construction materials[1–5], owing to its chemical stability, UV resistance, and capability of self-cleaning[6]. Over the past two

[1]Department of Civil Engineering, Jamia Millia Islamia, New Delhi, India. [2]School of Architecture and Design, K.R. Mangalam University, Gurugram, India. [3]Department of Civil Engineering, Delhi Technological University, New Delhi, India. [4]Department of Civil Engineering, Aligarh Muslim University, New Delhi, India. [5]Civil and Architectural Engineering Department, College of Engineering and Computer Sciences, Jazan University, PO Box 706, 45142 Jazan, Saudi Arabia. [6]Civil Engineering Department, College of Engineering, King Khalid University, 61421 Abha, Saudi Arabia. [7]Department of Civil Engineering, Malla Reddy (MR) Deemed to be University, Medchal-Malkajgiri, Hyderabad, Telangana 500100, India. [8]Faculty of Civil Engineering, Al-Furat University, Deir ez-Zor, Syria. ✉email: ahkhan@jazanu.edu.sa; ahmd.yaseen1993@gmail.com

decades, the integration of nanomaterials into traditional cement-based composites has garnered significant research interest due to their capability to improve mechanical performance, durability, and sustainability. The construction industry, which is responsible for 7–8% of global $CO_2$ emissions, faces increasing pressure to develop sustainable alternatives to conventional cementitious materials[7]. With an annual global consumption of nearly 30 billion metric tons of concrete[8], reducing the carbon footprints due to cement production is imperative. The widespread use of Ordinary Portland Cement (OPC) significantly contributes to environmental concerns, as producing one ton of OPC results in substantial $CO_2$ emissions[9]. Moreover, OPC is a major contributor to global $CO_2$ emissions, accounting for 5–10% of the annual total[10,11]. Without decisive intervention, industry emissions are projected to rise by 40% by 2050[12], underscoring the urgent need for comprehensive decarbonization strategies. Figure 1 shows the proportion of $CO_2$ emissions in various industries, highlighting the contribution of the cement sector. Addressing these challenges necessitates innovative material solutions, and nanotechnology offers a transformative approach by enhancing the working and longevity of the cement composites using different supplementary cementitious materials (SCMs), such as granulated blast-furnace slag (GBFS), fly ash (FA) and natural pozzolans, not only reduces the consumption of OPC, but also reduces the cost of concrete[13,14]. Moreover, SCMs could easily combined with other recycled materials for more valuable materials[15–17].

In the construction sector, NT plays a crucial role in enhancing the durability, aesthetics, and functionality of binding materials like cement[18]. It serves as an effective white pigment in coatings and decorative finishes, offering protection against UV degradation and atmospheric pollutants. Moreover, its incorporation into pavement materials contributes to air purification by breaking down vehicle-emitted pollutants, making it a promising candidate for sustainable and environmentally responsive infrastructure. The integration of nanotechnology into cement-based materials has revolutionized the construction industry, offering enhanced mechanical properties, durability, and sustainability. Among various nanomaterials, NT has emerged as a promising additive due to its unique physicochemical properties and multifunctional benefits[19]. NT particles are widely recognized for their ability to modify cement hydration kinetics, refine pore structure, and enhance durability characteristics. Although NT itself does not exhibit pozzolanic reactivity, its high surface area allows it to act as a nano-filler, promoting denser microstructures and improved mechanical performance[19]. The NT significantly influences the workability, hydration rate, and rheological behavior of cementitious systems, necessitating a comprehensive understanding of its effects on both fresh and hardened properties[6].

Several studies have highlighted the hydration-accelerating effects of NT, where it provides additional nucleation sites, leading to an earlier and more intense peak in the heat of hydration. The inclusion of NT has been found to increase early-age strength but decrease the setting time, yet higher dosages may adversely impact workability and long-term performance. Researchers such as Joshaghani et al. and Çelik et al.[20,21] have reported a significant reduction in slump flow due to NT's high water absorption tendency. Nevertheless, appropriate superplasticizer dosage and materials used as partial replacement of the cement, such as fly ash and slag, can mitigate workability challenges while further enhancing the durability and mechanical properties of NT-modified concrete[20–22].

The mechanical performance of NT-incorporated concrete has been widely investigated. Studies indicate that optimal NT dosages (typically ≤ 4 wt%) yield substantial strength enhancements at both early and later curing ages. For instance, Meng et al.[23] observed a 46–47% increase in 1-day compressive strength (CS) for concrete with 5–10% NT, although 28-day CS reductions were noted at higher dosages. Additionally, the optimal NT particle size (5 nm) exhibited superior CS gains (up to 24.35%) compared to larger NT particles[24]. Flexural and split tensile strengths (FS and STS) also improved significantly at moderate NT dosages (~ 1–5%), reinforcing its potential for high-performance concrete applications[25].

From a microstructural perspective, NT contributes to three primary modification mechanisms within the cement matrix. First, it works as a nucleation site, promoting the formation of needle-like hydration products

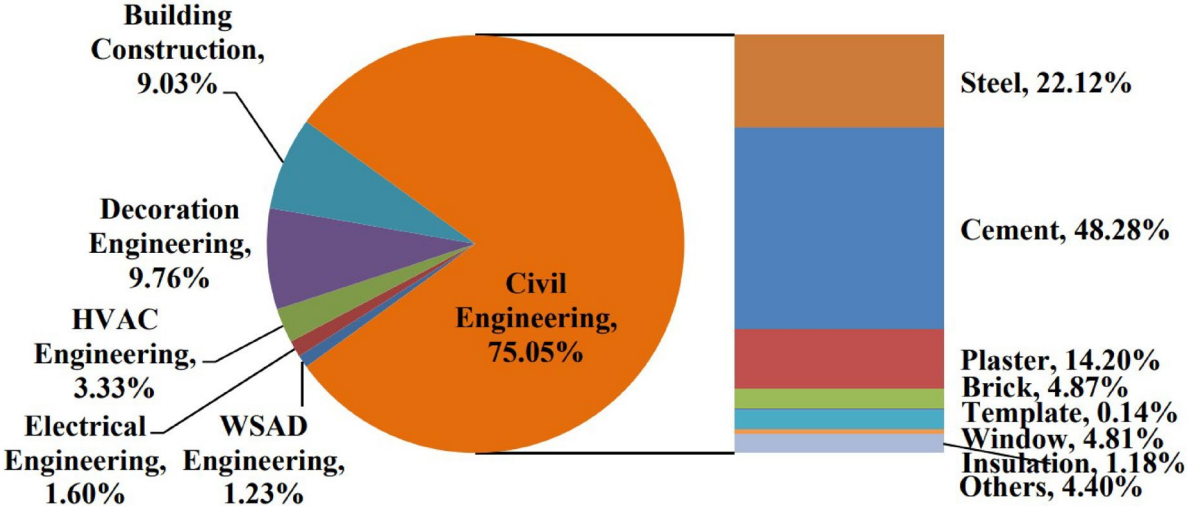


**Fig. 1**. Proportion of $CO_2$ emissions in various industries and the participation of cement in $CO_2$ emissions[30].

which fill capillary pores. Second, it facilitates the generation of more homogeneous and dense layers of calcium-silicate-hydrate (C-S-H) gel[26], which is crucial for strength development. Third, NT serves as a crystallization center for calcium hydroxide (CH), effectively refining paste-aggregate interfaces and improving mechanical interlocking. However, excessive NT content can result in unfavorable calcium titanate ($CaTiO_3$) formation, potentially compromising long-term durability[25,27]. This not only contributes to increased strength and durability but also introduces novel functionalities such as self-healing and electrical conductivity. Apart from these advantages, challenges persist in fully understanding the behavior of nanomodified cementitious materials, particularly concerning chemical resistance, tensile properties, and long-term structural stability.

Beyond mechanical and microstructural properties, NT enhances durability performance by reducing permeability, mitigating chloride ingress, and improving corrosion resistance. The incorporation of NT up to 1–3 wt% effectively reduces capillary absorption and water permeability, while excessive dosages can lead to agglomeration and decreased efficiency[27]. NT-modified concrete demonstrates notably lower chloride penetration, with reductions of up to 60% compared to control specimens[21]. Similarly, electrical resistivity measurements indicate a negligible corrosion rate at 90 days for NT-containing specimens[28], highlighting its potential in aggressive environmental conditions. However, more study are required to assess the long-term implications of CH accumulation, particularly in relation to durability aspects such as sulfate attack resistance and carbonation susceptibility. NT has also demonstrated remarkable resistance to environmental degradation, including acid attacks, carbonation, and high-temperature exposure. The thermal stability of concrete is an analytical factor in ensuring the structural integrity of buildings and infrastructure exposed to high temperatures. Studies have demonstrated that the influence of NT into cementitious composites significantly influences their performance under elevated temperatures. Farzadnia et al.[29] reported that NT-modified concrete exhibited enhanced residual CS, increased brittleness, and higher gas permeability compared to conventional concrete when exposed to 600 °C temperature. These findings highlight NT's impact on the microstructural evolution of cement-based materials under thermal stress. While NT contributes to strength retention at high temperatures, its influence on brittleness and permeability necessitates further exploration to optimize its application in fire-resistant construction materials. Understanding these effects is essential for developing next-generation, thermally resilient concrete composites with improved durability and mechanical stability in extreme environments.

The inclusion of nanomaterials in cement-based systems presents a transformative approach to overcoming long-standing challenges in construction materials, such as brittleness, porosity, and chemical susceptibility. This research explores the role of NT in enhancing the mechanical, durability, and microstructural properties of cementitious materials, aiming to bridge the gap between fundamental nanotechnology and practical construction applications.

While previous studies have largely examined NT for early-age strength development or single durability aspects (e.g., chloride ingress or acid attack), there remains a lack of integrated investigations that concurrently address mechanical, microstructural, and durability performance under multiple aggressive exposures. Moreover, only a limited number of studies have investigated long-term curing (up to 180 days) and fire resistance, and even fewer have incorporated an economic feasibility analysis to justify practical implementation. This study fills this gap by presenting a holistic assessment of NT-incorporated concrete, correlating strength development with microstructural densification and durability indices, and further complementing these findings with cost–benefit analysis for real-world applicability.

This research advances the production of nano-engineered concrete by systematically investigating the mechanical, microstructural, and durability properties of NT-incorporated concrete composites. The study begins with an extensive evaluation of mechanical performance, assessing the influence of varying NT dosages (0.5%, 1%, and 1.5%) on compressive, tensile, and flexural strengths. To further understand the impact of NT at the nanoscale, microstructural analyses, including scanning electron microscopy (SEM) were conducted to examine the densification of the cementitious matrix, refinement of pore structure, and improved bond efficiency. The durability performance of NT-modified concrete was then rigorously assessed under aggressive environmental conditions. The nano-concrete was exposed to 4% sodium chloride, 4% hydrochloric acid, and 4% sulfuric acid for 90 days to evaluate their resistance to chemical deterioration. Additional durability tests, including alternate freeze-thaw cycles, rapid chloride penetrability, surface resistivity, and accelerated carbonation, were performed to determine long-term stability. The behavior of NT-incorporated concrete was further analyzed under elevated temperatures (200 °C, 400 °C, and 600 °C), alongside an assessment of its modulus of elasticity. Furthermore, non-destructive testing facilitated the development of empirical models for predicting compressive strength along with economic feasibility analysis. This comprehensive study establishes NT as an optimistic nanomaterial for enhancing the strength, microstructural integrity, and durability of concrete. The findings highlight the revolutionary capabilities of nanotechnology in advancing high-performance, resilient construction materials for modern infrastructure applications.

## Materials

### Cement

Ordinary Portland Cement (OPC), 43 grade, conforming to IS 8112 – 2013, was used. Its properties are listed in Table 1, meeting the required specifications[31]. Figures 2a and 3a show the physical appearance and microstructure of the cement used in the current study.

### Fine aggregate

Locally sourced Badarpur sand with a fineness modulus of 2.55 was used as fine aggregate (FA). It satisfied IS 2386 (Part 1): 2016 requirements[32] and the physical appearance and the gradation curve of FA is shown in Fig.

| S.No. | Properties | Values | Specified values as per IS 8112 – 2013 [31] |
|---|---|---|---|
| 1. | Consistency | 28.50% | – |
| 2. | Initial setting time | 61 min | > 30 min |
| 3. | Final setting time (minutes) | 294 | < 600 min |

**Table 1**. Properties of cement.


**Fig. 2**. Material used (**a**) cement, (**b**) Badarpur sand, (**c**) NT, and (**d**) superplasticizer.

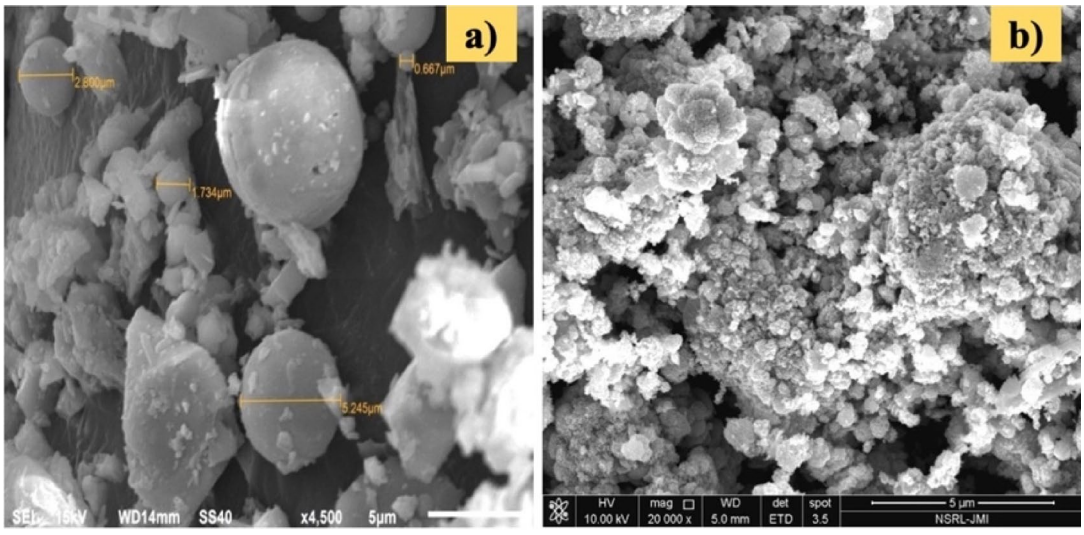


**Fig. 3**. Microstructure images of (**a**) cement (**b**) NT used.

2b and 4b, respectively. The FA exhibited a bulk density of 1620 kg/m$^3$, a specific gravity of 2.63, and a water absorption of 1.2%, confirming its suitability as a medium sand for concrete production. Prior to batching, the fine aggregate was conditioned to a saturated surface dry (SSD) state to account for its absorption capacity and ensure accurate control of the effective water-to-binder ratio.

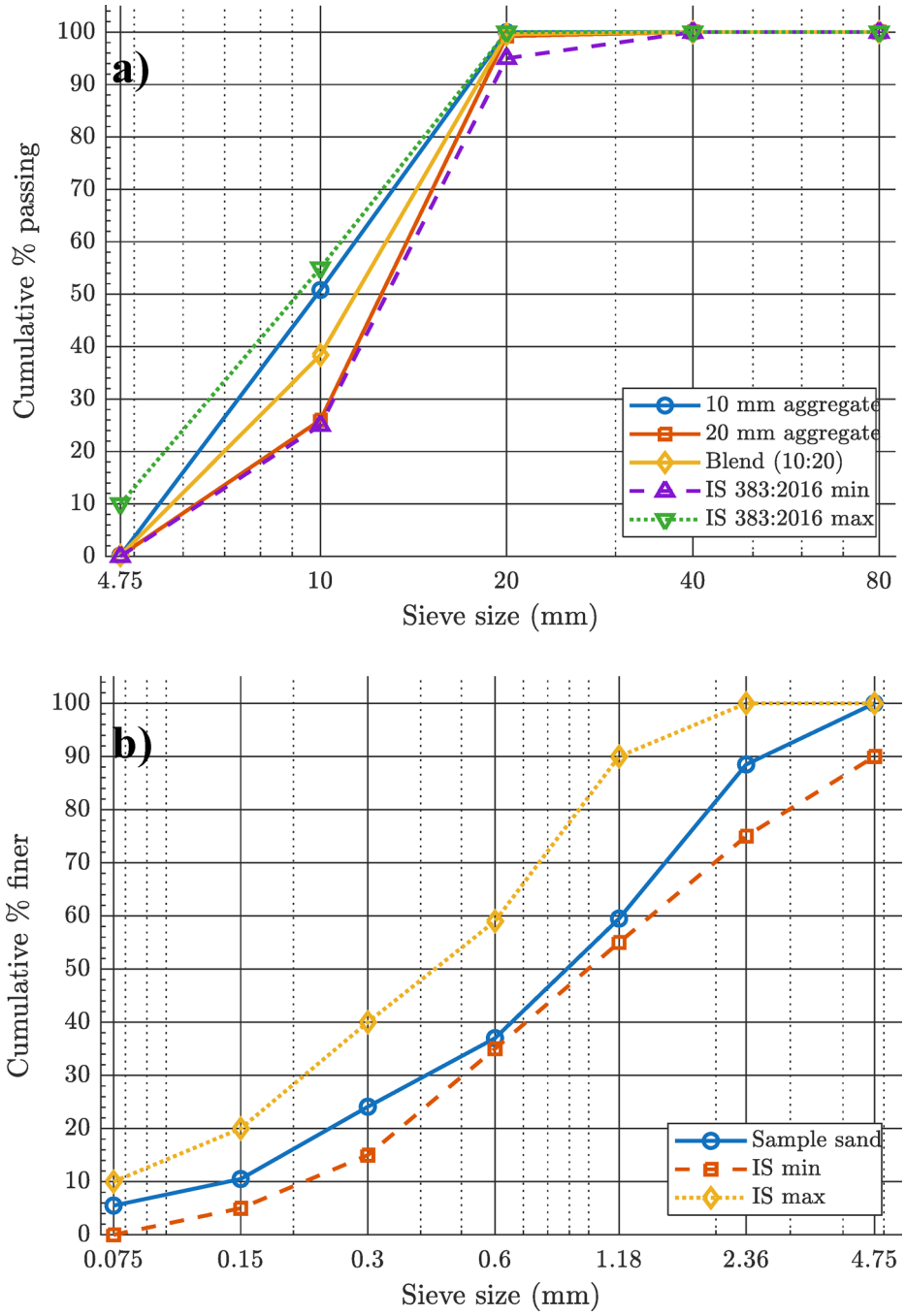


**Fig. 4**. Gradation curve of (**a**) CA and (**b**) FA.

### Coarse aggregate

Crushed granite aggregates of 10 mm and 20 mm sizes were used in a 60:40 blend, in accordance with IS 383:2016. The combined fineness modulus was 6.71[32,33]. Figure 4a show the gradation of the CA used in the current study, respectively. Physical characterization of CA includes a bulk density of 1520 kg/m$^3$, a specific gravity of 2.70, and a water absorption of 0.5%. The aggregate grading was verified through sieve analysis, and the results were within the specified limits for 20 mm CA. To avoid errors in mix water calculation, the coarse aggregate was brought to a saturated surface dry (SSD) condition prior to mixing.

### Water

Potable tap water, free from deleterious substances, was used for mixing and curing, as per IS 456–2000[34].

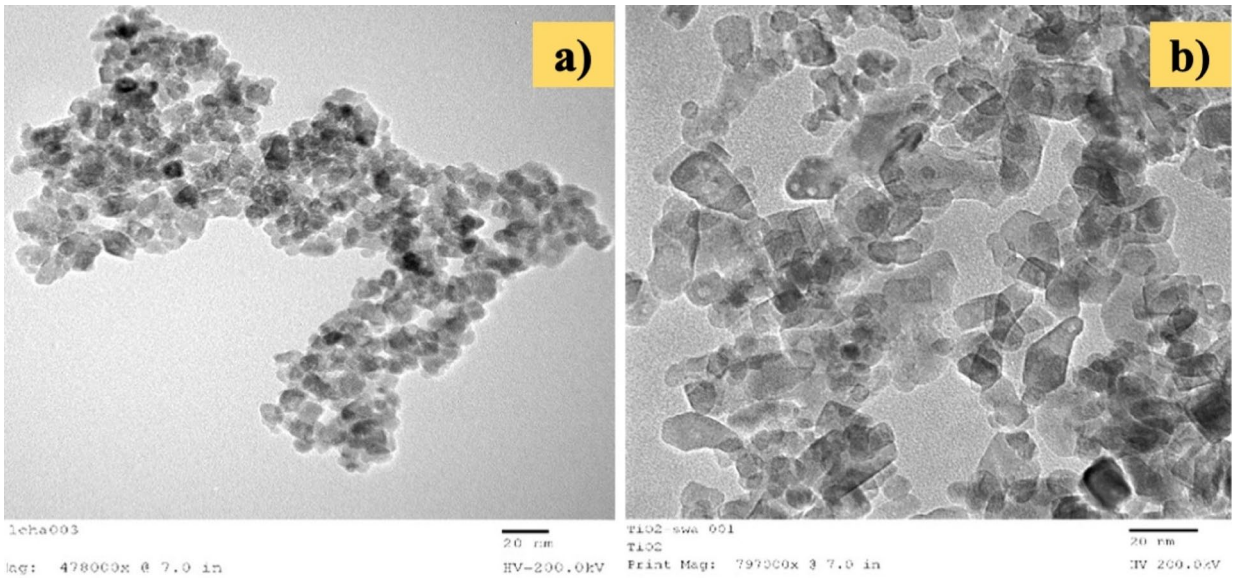


**Fig. 5**. TEM images of NT at (**a**) 60,000×, and (**b**) at 1,00,000×.

| Mix | Cement (kg/m$^3$) | NT (kg/m$^3$) | Fine aggregate (kg/m$^3$) | Coarse aggregate (kg/m$^3$) | Water (kg/m$^3$) | SP (kg/m$^3$) | W/C ratio | Ratio of mix |
|---|---|---|---|---|---|---|---|---|
| 0NT | 380 | 0 | 700 | 1310 | 87.4 | 3.8 | 0.23 | 1:1.84:3.44 |
| 0.5NT | 378.1 | 1.9 | 700 | 1310 | 87.4 | 4.18 | 0.23 | |
| 1.0NT | 376.2 | 3.8 | 700 | 1310 | 87.4 | 4.56 | 0.23 | |
| 1.5NT | 374.3 | 5.7 | 700 | 1310 | 87.4 | 4.94 | 0.23 | |

**Table 2**. Mix design used in the current study.

### Nano titanium dioxide

Commercially obtained NT from Evonik Industries (Frankfurt, Germany) with a BET surface area of ~ 45 m$^2$/g and particle size of 6–18 nm (average 10.2 nm; D10 = 7.5 nm, D50 = 9.8 nm, D90 = 14.8 nm) was used. The physical appearance and microstructure of the NT is shown in Figs. 2c and 3b respectively. TEM analysis confirmed narrow size distribution (6–18 nm), favoring improved nucleation and densification as shown in Fig. 5a–b. According to a previous study, NT consists predominantly of anatase (76%) with rutile (11%) and trace brookite[35].

The size of nanoparticles rises with the increase in reaction temperature. Some researchers noticed that particle size is affected by the loading of precursor, not the reaction temperature[36].

### Superplasticizer

A polycarboxylate ether (PCE)-based superplasticizer (% by cement mass) (MasterGlenium SKY 8233, BASF; solid content 35%) was used to maintain workability (see Fig. 2d), conforming to IS 1199–1959. The SP dosages at 1%, 1.11%, 1.21%, and 1.32% have been used in the GPC mix with 0%NT, 0.5%NT, 1%NT, and 1.5NT respectively.

## Methodology

A comprehensive experimental investigation was conducted to assess concrete properties in its fresh and hardened state, incorporating NT. The study focused on M40 grade concrete, incorporating varying NT dosages of 0.5%, 1%, and 1.5%, with results benchmarked against conventional M40 concrete. For clarity in designation, the conventional concrete mix was labeled 0NT, while the NT-modified mixes were designated as 0.5NT, 1NT, and 1.5NT, corresponding to their respective NT content. The mix proportion details for M40 concrete are presented in Table 2.

The concrete was prepared following a controlled mixing sequence to ensure proper dispersion of NT and uniformity of the mix. First, the coarse aggregates and fine aggregates were introduced into a pan mixer and dry-mixed for 2 min. Cement was then added and mixed for another 2 min to obtain a homogeneous dry blend. In parallel, the required dosage of NT was dispersed in the mixing water using a high-shear mechanical disperser operating at ~ 2000 rpm for 10 min, which helped to minimize agglomeration of nanoparticles. The NT dispersed solution was then slowly added to the dry mix while the mixer was running. Finally, the superplasticizer was added, and the mixing continued for an additional 3–4 min until a uniform and workable concrete mix was achieved. This procedure ensured stable dispersion of NT within the cementitious matrix. It is essential to note

that, although the water-to-cement ratio for all concrete mixes was maintained at 0.23 (Table 2), a higher water-to-cement ratio of 0.40–0.45 was specifically adopted for mortar cube testing to ensure workability, as per IS 4031.

## Testing procedures

*Compressive strength of cement mortar*

For mortar cube testing, potable tap water was used for the preparation of the matrix as well as for curing. The ratio of the cement to fine aggregate was maintained at 1:3 by weight. A higher water-to-cement ratio of 0.40–0.45 was adopted in mortar mixes to ensure adequate workability for casting 70.06 mm cubes, in line with IS 4031 (Part 6). It should be noted that this differs from the water-to-cement ratio used for concrete mixes, as the mortar tests were intended for preliminary paste–aggregate interaction assessment rather than structural concrete evaluation.

*Slump test*

The workability of fresh concrete mixtures was assessed via slump testing in accordance with IS 1199–1959 (reaffirmed in 2013)[37], measuring consistency and flow characteristics under gravitational settlement. A control mix was designed for a target slump of 100–110 mm, suitable for M40 grade concrete, while NT incorporation was evaluated for its influence on rheological performance. Prior to concrete testing, samples were prepared to examine the binding capacity of the nano-enhanced cementitious matrix—a critical factor governing composite strength. Samples were fabricated using a 1:3 cement-to-fine aggregate ratio per IS 4031-6:1988 and IS 8112:2013[31,38], cured in potable water, and tested under compressive loading to assess matrix strength development.

*Petrographic analysis*

To examine the microscopic properties of the prepared cement matrix, the cement mortar cubes were cast and tested under the compression Testing Machine (CTM) and are now studied under a microscope. After testing, the cube pieces are converted into thin microscopic slides, as shown in Fig. 6, to study under a microscope.

To achieve the testing under the microscope, the thick pieces of the cement cubes were first grind to fine particles and stuck on the glass to make a slide. The slide of different proportion of NT added to the cement cubes was prepared, as shown in Fig. 6b, and kept under a microscope for investigation.

*Compressive strength test*

The CS test for the normal concrete mix and NT-based concrete mix was done according to IS 516–1959 (Reaffirmed in 2021)[39]. A total of 48 cube specimens (150 mm) were prepared for the CS test, as shown in Fig. 7a–b. For each mix (0NT, 0.5NT, 1NT, and 1.5NT), 12 cubes were cast. These were equally divided for testing at four curing ages (7, 28, 90, and 180 days), i.e., 3 cubes per mix per age. The average of three specimens was reported as the compressive strength at each age. Before testing these concrete specimens, the cube's surfaces were first dried and then put in the CTM with a loading rate of 0.25 MPa/s (approximately equivalent to 2.5 KN/s) until failure, as shown in Fig. 8a.

*Split tensile strength test*

The split tensile strength (STS) test of the normal mix concrete and NT-based concrete was done as per IS 5816 – 1999 (Reaffirmed in 2004) to assess its tensile strength[40]. For STS, 12 cylindrical specimens (100 × 200 mm) were cast as shown in Fig. 7c. Although IS 5816 – 1999 commonly specifies 150 × 300 mm cylinders, the reduced-size specimens were adopted in this study due to ease of handling and to optimize material use.


**Fig. 6**. The slides prepared for different dosages of NT for microscopic investigation.

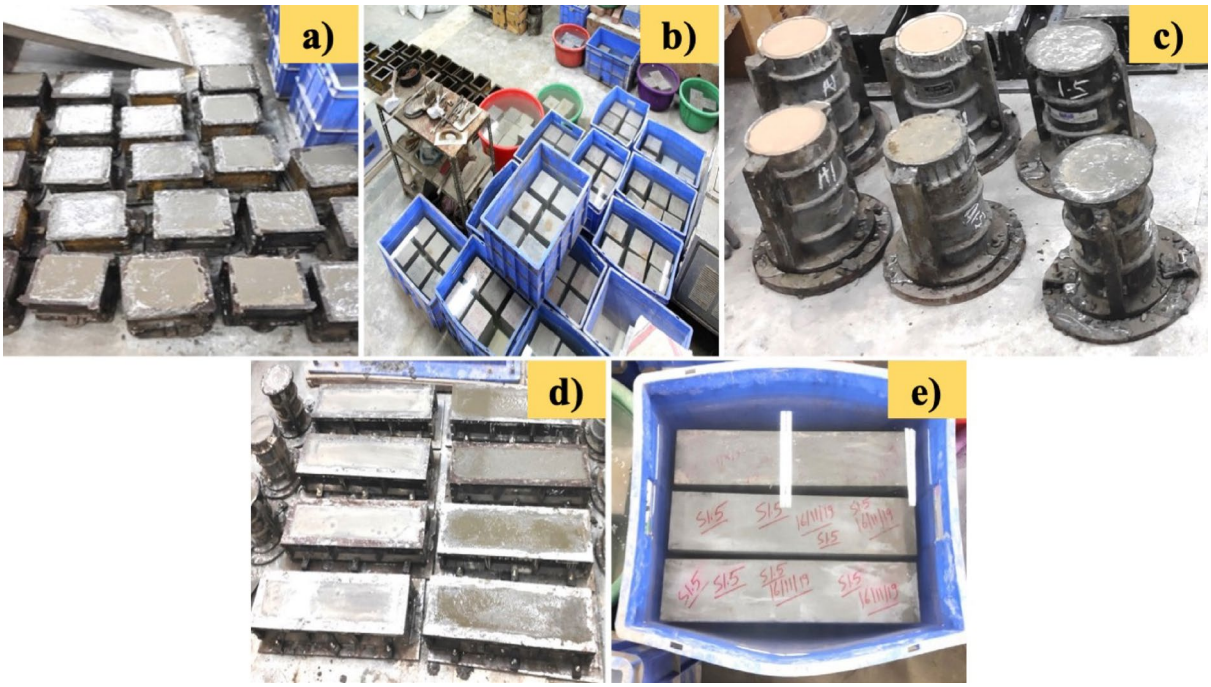


**Fig. 7**. (**a**) Casted specimen for CS, (**b**) curing of casted specimen, (**c**) casted concrete cylinders for STS testing, (**d**) specimen casted for FS test, and (**e**) curing of casted beams.


**Fig. 8**. Testing of casted specimens (**a**) CS Test, (**b**) STS Test, and (**c**) FS Test.

The chosen dimensions comply with ASTM C496 and are widely reported in the literature for indirect tensile strength testing[41], as they preserve the standard aspect ratio of 2.0. Therefore, the conversion of applied load to STS remains valid and comparable with standard results For each mix (0NT, 0.5NT, 1NT, and 1.5NT), 3 cylinders were tested at 28 days in the CTM under diametral compression at a loading rate of 1.2–2.4 MPa/min (approximately equivalent to 2 KN/s) until splitting failure occurred as shown in Fig. 8b. The average of three results was reported.

*Flexural strength test*

A beams of size 100 mm in breadth,100 mm in width, and 500 mm in length were used for evaluation of flexural strength (FS). The test was conducted as per IS 516–1959 (reaffirmed in 2004)[39]. A total of 12 prismatic beams were cast for FS testing. For each mix, 3 beams were tested at 28 days, and the mean value was reported, as shown in Fig. 7d, and were demoulded after 24 h and placed underwater for curing, as shown in Fig. 7e for 28 days. After 28 days, the rectangular prism beams were taken out from the curing tank, and their facade was wiped with a piece of cloth for testing. Two-point loads were applied on a rectangular prism beam's top surface to test the

rectangular prism beam, as shown in Fig. 8c. The effective span was set to 400 mm, measured centre-to-centre between the support rollers, giving a span-to-depth ratio L/d = 4.0. The two loading noses were positioned at L/3 from each support (i.e., 133.3 mm from the nearest support), creating a constant-moment region over the middle third of the span. The shear span a (support to nearest load point) was therefore a = L/3(133.3 mm), giving a/d = 1.33. Supports and load noses were steel rollers allowing free rotation; bearing strip widths conformed to the standard. The load was applied at a constant rate of 0.06 MPa/s (approximately equivalent to 1.8 KN/min) until failure.

*Rebound hammer test (non-destructive testing)*
Rebound Hammer (RH) test was performed on normal mix concrete and NT based-concrete according to IS 13,311 Part 2-1992 (reaffirmed in 2004)[42]. For RH, 12 cube specimens (150 mm) were cast and cured for 28 days. Each mix had 3 cubes, tested on multiple faces, and the average rebound number was compared with compressive strength values. Consequent to curing, the surface was dried with cloth, as discussed in the compressive strength test, and the prepared cubes were then tested with a Schmidt Rebound Hammer, as shown in Fig. 9a.

*Ultra-sonic pulse velocity test (non-destructive testing)*
Ultra Sonic Pulse Velocity (UPV) test was performed as per IS 13,311 Part 1-1992 (reaffirmed in 2004) on concrete cubes with and without NT[43]. A Portable Ultrasonic Non-destructive Digital Indicating Tester (PUNDIT Lab) was used. The test employed a pair of 54 kHz longitudinal transducers, which are standard for concrete quality assessment. Petroleum jelly was applied at the transducer surface interface as a coupling medium to ensure effective transmission of ultrasonic pulses. Measurements were taken using the direct transmission method, with the transducers placed on opposite faces of the specimen. The same 12 cubes used for RH were employed for UPV testing (3 cubes per mix at 28 days) as shown in Fig. 9b. The average pulse velocity was reported for each mix.

*Microstructure analysis*
Scanning electron microscope (SEM) analysis on the NT-based concrete matrix was also carried out to assess the matrix's behavior at the nano-scale. Small fragments of concrete from compressive strength test cubes (post-failure) were used for SEM and petrographic studies, as shown in Fig. 10a. Thus, no additional specimens were cast exclusively for microstructural analysis. The coated samples were then placed in the SEM machine to get the NT-based concrete matrix's morphology, as shown in Fig. 10b.

*Durability analysis*
Durability test: concrete exposure to harmful chemicals The durability of concrete is a crucial parameter that defines its ability to withstand chemical attacks, particularly from aggressive substances such as sodium chloride (NaCl) present in the surrounding environment. The present investigation focuses on evaluating the influence of nano additives and their composites on the durability performance of concrete when exposed to a chemically aggressive environment. For this purpose, a total of 36 concrete cubes of M40 grade, both with and without NT, were cast and designated properly for identification. The freshly cast specimens were demoulded after 24 h and subsequently submerged in a saline solution containing 4% NaCl, 4% HCl, and 4% $H_2SO_4$ by weight for different exposure durations of 7, 28, and 90 days to simulate prolonged chemical attack conditions. Specimens were fully submerged in the aggressive solutions throughout the exposure period. The solutions were renewed every 7 days to maintain chemical concentration, and pH was monitored weekly (maintained within ± 0.2). The exposure was conducted at laboratory temperature (27 ± 2 °C). Before compressive strength testing, the specimens were gently


**Fig. 9**. Non-destructive test (**a**) RH, (**b**) UPV.


**Fig. 10**. (**a**) Gold coated samples for SEM, and (**b**) SEM machine.

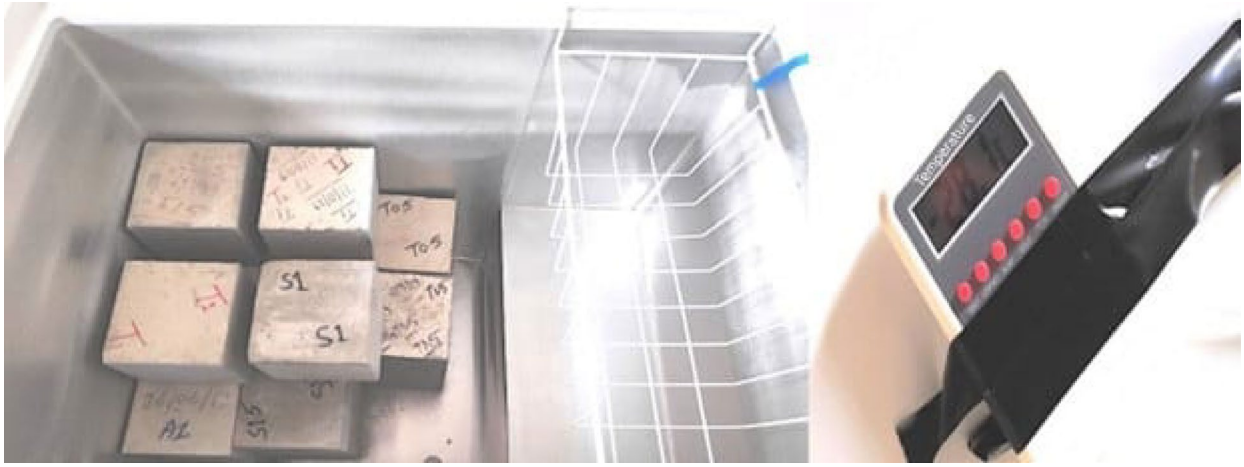


**Fig. 11**. Concrete cubes in the refrigerator for freezing at −28 °C.

rinsed with distilled water and surface-dried to avoid residual chemicals influencing the results. Therefore, the concrete specimens were removed from the solution, surface-dried, and tested using a CTM until complete failure (collapse). The results obtained from this test provide insights into the resistance of concrete against chemical degradation, thereby helping to assess the effectiveness of nano additives in enhancing durability and long-term performance in aggressive environments.

Durability test: concrete exposure to alternate freeze-thaw The freeze–thaw resistance of NT-modified and control concretes was evaluated in accordance with the guidelines of ASTM C666 [44]. Concrete cubes (150 mm) were cured for 28 days in water and then subjected to 120 freeze–thaw cycles. Each cycle consisted of 24 h freezing at −28 ± 2 °C, followed by 24 h thawing at 27–30 °C (see Fig. 11). The specimens were fully saturated prior to exposure, and their compressive strength was measured at the end of the exposure period. Three cubes per mix were tested, and the average was reported. In addition to compressive strength, the freeze–thaw durability was evaluated using multiple indices, including mass loss, dynamic modulus change, visual damage index (VDI), and compressive strength loss per cycle. The mass of specimens was recorded before and after 120 cycles, and percentage mass loss was calculated. Relative Dynamic Modulus of Elasticity (RDME) was derived from UPV values before and after cycles using ASTM C666 equation. A visual damage index (0 = intact, 1 = minor surface scaling, 2 = moderate cracking, 3 = severe spalling) was used based on specimen appearance. CS loss per cycle was obtained by dividing the total CS reduction by the number of cycles.

Durability test: accelerated carbonation test This test was conducted to ascertain the durability of the NT-based concrete. For that, samples were cast with M40 grade (with and without NT) and were cured for a specified 28 days. After curing was completed, the concrete specimens were kept in a carbonation chamber. For the

accelerated carbonation test, specimens were exposed to 2% $CO_2$ concentration, 65 ± 5% relative humidity, and 27 ± 2 °C for 30 days. After exposure, specimens were split to obtain fresh cross-sections, and a 1% phenolphthalein alcohol solution was sprayed immediately. The depth of carbonation was measured as the distance from the exposed surface to the colorless zone, using a digital Vernier calliper with 0.01 mm accuracy. For powdered sampling, the outer surface layer was removed in increments of 1 mm thickness using a rotary grinder. The collected powder was tested with phenolphthalein to confirm the depth of carbonation. Each reported value is the average of three measurements per specimen. To induce smooth carbonation of all the concrete specimens at the time of carbonation acceleration, enough space was provided between each concrete specimen to ensure that the specimen's contact with the air could be smoothly maintained.

Durability test: surface electrical resistivity test The surface resistivity of concrete was measured according to AASHTO TP 95 using the four-point Wenner probe method[45]. Cylindrical specimens (100 × 200 mm) were cast and water-cured for 28 days. Prior to testing, the cylinders were saturated in limewater for 24 h to maintain consistent moisture content (see Fig. 12), as resistivity is strongly influenced by pore saturation. Measurements were taken at 23 ± 2 °C by placing the probe on four different quadrants of the specimen surface, and the average of the readings was reported for each mix.

Durability test: rapid chloride penetration test (RCPT) RCPT test is also an indirect test for measuring concrete permeability. RCPT was conducted according to AASHTO T277[46] and ASTM C1202[4]. Cylindrical specimens (100 mm dia. × 200 mm) were cast and water-cured for 28 days. After curing, the cylinders were cut into 50 mm-thick discs. The specimens were vacuum-saturated in limewater for 24 h before testing to ensure full pore saturation. Each disc was then mounted in the test cell, with one side exposed to 3% NaCl solution and the other to 0.3 N NaOH solution. A constant DC potential of 60 V was applied across the specimen for 6 h at a test temperature of 23 ± 2 °C, and the total charge passed (coulombs) was calculated. The cylindrical specimen's side is coated with epoxy or with electric tape, as shown in Fig. 13a.

It is then installed in the test apparatus, as shown in Fig. 13b. The test cell's left-hand side (negative terminal) is filled with a 3% NaCl solution, while the right-hand side (positive terminal) contains a 0.3 N NaOH solution. After setting up the system, a voltage of 60 volts is applied for a duration of six hours, with measurements


**Fig. 12**. SR test using a four-point Wenner probe.

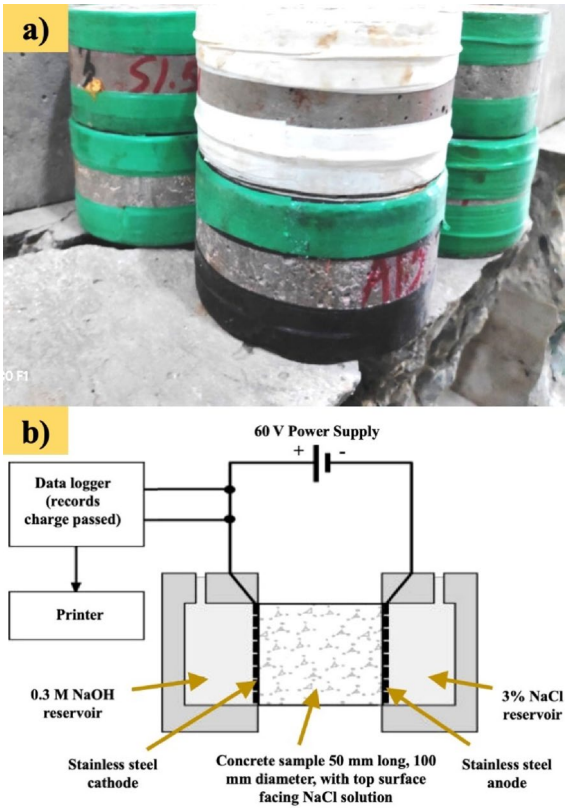


**Fig. 13**. (**a**) Concrete cylinder specimen of 50 mm by 100 mm for RCPT and (**b**) AASHTO T277 (ASTM C1202) test setup[47].

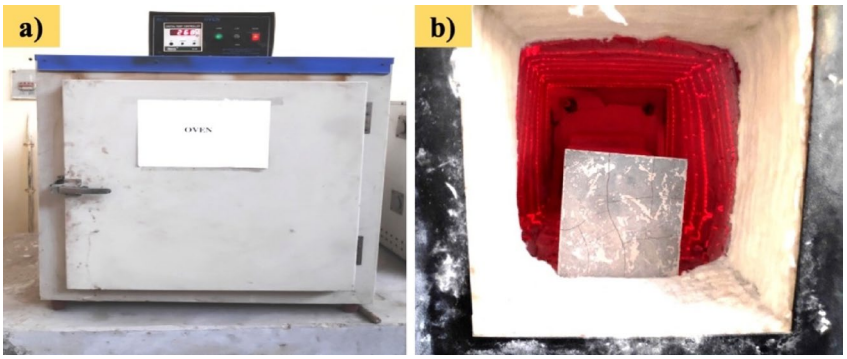


**Fig. 14**. (**a**) Concrete specimens under oven drying at 300 °C and (**b**) concrete specimens subjected to fire in a muffle furnace.

recorded every thirty minutes. Once the six-hour period concludes, the specimen is removed from the cell, and the total number of coulombs passing through the sample is calculated. The resulting data are then compared against the specifications outlined in AASHTO T277-83 and ASTM C1202[46,47].

Durability test: concrete exposure to oven drying at 300 °C To evaluate the NT based concrete matrix under the influence of thermal stresses due to oven drying of the concrete cubes at 300 °C (see Fig. 14a). For the test, the cubical sample of 150 mm size is casted, demoulded after 24 h and curing of the concrete cubes was conducted for 28 days. Concrete cubes after 28 days of curing were taken out from the curing tank and were left for some hours in the environment so that the surfaces of the cubes were dried. As soon as the cubes' surfaces were dried, the concrete specimens were kept inside the Oven for 24 h at 300 °C, as shown in Fig. 14a.

After 24 h of oven drying at 300 °C, the oven power was disconnected, and the gate of the Oven was opened to cool down the concrete specimens. As soon as the concrete specimens were cool down to normal after some time, the concrete specimens were then placed under CTM to get the CS.

Durability test: concrete exposure to fire at 200 °C, 400 °C, and 600 °C To analyse the concrete performance against the fire, 36 nos. of M40 grade concrete cubes of 100 mm were cast. The reason for casting 100 mm small concrete cubes instead of 150 mm concrete cubes was the muffle furnace's small mouth size. The cubes were removed from the moulds after 24 h and placed in a water tank for curing over a period of 28 days. After the curing period, the cubes were taken out of the tank and air-dried for 24 h. Once the surfaces had dried, the cubes were then oven-dried at 100 °C for an additional 24 h to eliminate any remaining moisture from the concrete.

After oven drying for 24 h, the cubes were finally kept in the muffle furnace, as shown in Fig. 14b, for about 6 h to assess the concrete's resistance against fire at high temperatures. i.e., 200 °C, 400 °C, and 600 °C. After heating at different temperatures for 6 h, the cubes were then allowed to cool down at room temperature. As soon as the cubes' surface was cooled down, the cubes were subjected to CTM to assess the CS of the concrete matrix.

Durability test: capillary porosity test The capillary porosity test was also conducted on NT based concrete matrixes to assess the pores and voids present in the concrete's internal structure. The concrete cubes of M40 grade were cast with M40 grade (with and without NT), demoulded, and cured for 28 days. Cured concrete specimens after 28 days were taken out and were air-dried for 24 h. After the surface becomes dry, the cubes were then placed in the oven for oven drying at 100 °C for another 24 h to wipe out the moisture from the concrete cubes. After oven drying for 24 h, the cubes were finally kept in the water reservoir again so that the half surface of the cube submerged in water and the remaining half portion free in the environment, as shown in Fig. 15a. This test was conducted for about one month, and no capillary movements of water through pores were observed within the concrete for the normal mix as well as the concrete mixed with NT. The half portion of the concrete cube, free in the environment, remains dry even after a month, as shown in Fig. 15b. On the other hand, in the same manner mentioned above, the concrete cube of M25 grade was submerged (see Fig. 15c) to draw a comparison between the two mixes. The capillary action through pores was evident in the M25 grade concrete as water moves up to the cube's top surface, making the whole concrete cube wet, as shown in Fig. 15d within three days.

Durability test: permeability test The concrete cubes of M40 grade were cast with M40 grade (with and without NT, demoulded, and cured for 28 days. The test was conducted for more than a month at a pressure head of 15 kg/cm$^2$ as per IS: 3085 – 1965 (reaffirmed in 2002) code[48], as shown in Fig. 16a–b. Flow through the specimen was measured volumetrically over a 24 h interval. The coefficient of permeability, k, was calculated from Darcy's law using Eq. 1. The permeability apparatus used has a detection limit of $1 \times 10^{-12}$ m/s.

$$k = \frac{Q * L}{A * t * H} \tag{1}$$

where Q is the total volume of flow (m$^3$), L is the specimen thickness (m), A is the cross-sectional area (m$^2$), t is the measurement time (s), and H is the applied hydraulic head (m).

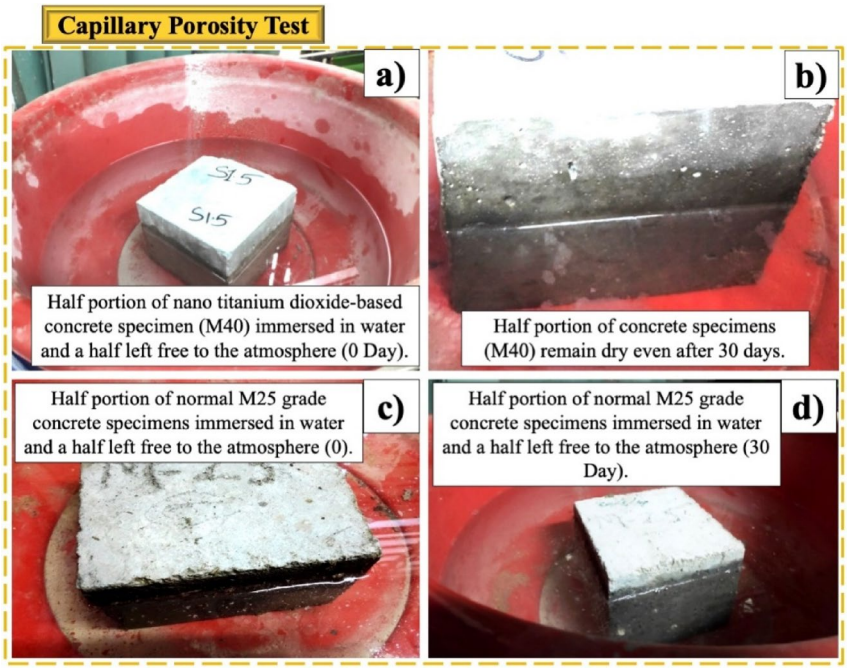


**Fig. 15**. Half portion of concrete specimen immersed in water and half left free to the atmosphere: (**a**) M40 nano titanium dioxide-based (0 days), (**b**) M40 nano titanium dioxide-based (30 days), (**c**) normal M25 grade (0 days), and (**d**) normal M25 grade (30 Days).

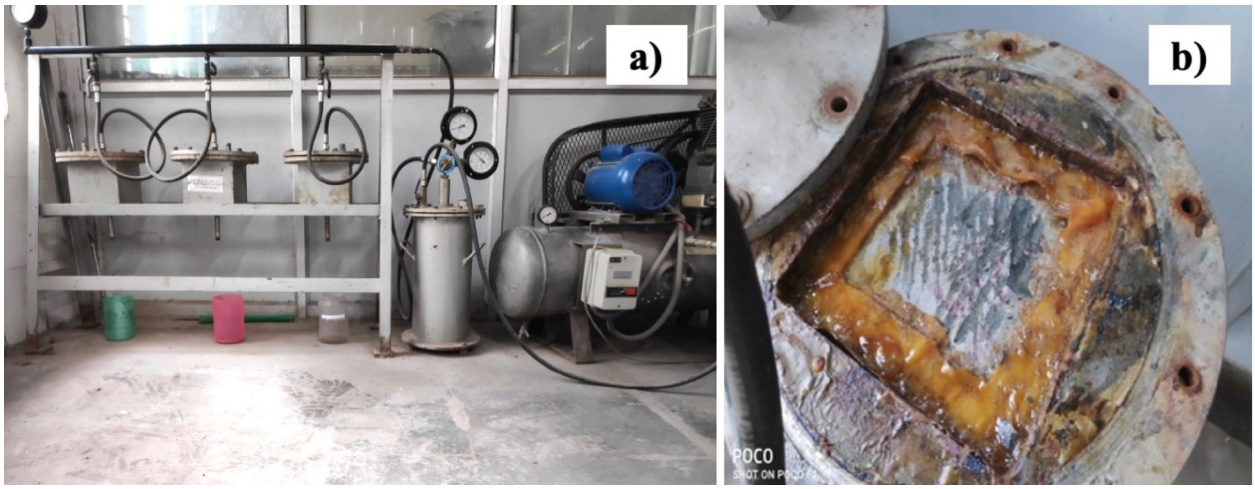


**Fig. 16**. (**a**) Water permeability test apparatus and (**b**) concrete cube specimen placed in water permeability test apparatus.

| Cube designation | Compressive strength 28 days (MPa) |
|---|---|
| 0NT | 45.75 |
| 0.5NT | 47.00 |
| 1NT | 49.20 |
| 1.5NT | 50.50 |

**Table 3**. Compressive strength of cement mortar cured for 28 days.

| Mix designation | Slump value (mm) | Decrease in the slump (%) |
|---|---|---|
| 0NT | 100 | – |
| 0.5NT | 84 | 16 |
| 1NT | 72 | 28 |
| 1.5NT | 64 | 36 |

**Table 4**. The result of the slump test.

## Results and discussion

### Compressive strength of cement mortar

The compressive strength of the cement paste cubes of normal mix, using different dosages of NT, cured for 28 days, is given in Table 3. The compressive strength of the cement mortar increases by 2.73%, 7.54%, and 10.38% after incorporating 0.5%, 1%, and 1.5% NT, respectively, in comparison with the control the cement mortar. This enhancement in the strength property of cement mortar is due to the filling of cracks at the nano scale after the incorporation of NT and the formation of an extra layer of hydrate gels.

### Workability

The workability of the fresh concrete mix incorporating NT was evaluated through the slump test, with the results presented in Table 4. The recorded slump values for mixes containing 0.5 wt%, 1 wt%, and 1.5 wt% NT were 84 mm, 72 mm, and 64 mm, respectively. The observed reduction in workability can be attributed to the high surface area of NT particles[19], which increases water demand within the mix due to enhanced particle interactions and a higher degree of cementitious material hydration.

Zhang et al.[8] observed a 2.8–20.8% decrease in workability with the incorporation of 1–5 wt% NT, demonstrating a consistent decline in slump values with increasing NT content. Although setting time measurements were not directly performed, the reduction in slump retention suggests an accelerated hydration process and reduced flowability with higher NT content. Previous studies have reported similar trends, attributing this to the nucleation effect of NT, which enhances the early hydration of cementitious phases[19]. To address the increased water demand and reduced slump retention, adjustments to the water-to-cement ratio or the use of superplasticizers are recommended when incorporating NT into concrete mixtures.

In the present study, the reduction in workability was effectively managed by incorporating an additional dosage of superplasticizer to maintain the desired consistency. The results of the slump test are further illustrated in Fig. 17. The reduction of workability on the addition of NT can be accounted for by hydration reactions and particle interactions with the cementitious system. The following are the chief mechanisms involved:

*Increased hydration rates*
NT acts as a nucleation site, accelerating the tricalcium silicate ($C_3S$) and dicalcium silicate ($C_2S$) hydration reaction of the cement. The rapid growth of the calcium silicate hydrate (C-S-H) gel is the result, trapping free water and reducing workability (Eqs. 2–3):

$$2C_3S + 6H_2O \rightarrow 3C - S - H + 3Ca(OH)_2 \quad (2)$$

$$2C_2S + 4H_2O \rightarrow 3C - S - H + Ca(OH)_2 \quad (3)$$

*Increased water demand*
Due to its high surface area, NT can absorb water molecules, hence reducing the free water for workability (Eq. 4):

$$2C_2S + 4H_2O \rightarrow 3C - S - H + Ca(OH)_2 \quad (4)$$

*Agglomeration effect*
The strong van der Waals forces among the NT particles result in particle agglomeration, increasing the viscosity of the blend and also reducing workability. When NT is added to a cementitious system, it interacts with $Ca^{2+}$ ions from cement hydration, forming secondary hydration products that further contribute to agglomeration (Eq. 5):

$$TiO_2 + H_2O \rightarrow TiO_2 \cdot H_2O \quad (5)$$

## Compressive strength (CS)

Each CS value in Table 5 represents the mean of three specimens, reported as mean ± standard deviation (SD) ($n = 3$). The inclusion of NT reduced data variability compared to the control, indicating more uniform matrix densification. The improvements, particularly at 1.5% NT, were statistically consistent across all curing ages. As shown in Table 5, the incorporation of NT in the concrete mix resulted in a significant rise in CS compared to the 0NT. Among the three dosages of NT tested, the highest increase in CS was observed at a 1.5% NT dosage, with an impressive 28.70% enhancement in strength after 28 days of curing. These results corroborate the findings of Jenima et al. [19], who also reported similar improvements in strength with NT incorporation. At the 0.5% NT dosage, the CS increase was 10.54%, while at 1% NT, the enhancement was 21.98%, both compared to the conventional mix (0NT) cured for 28 days.

This pattern of strength improvement was consistent across all curing durations. Specifically, the maximum CS values at 180 days of curing were 58.20 MPa, 64.50 MPa, 71.00 MPa, and 75.25 MPa for the 0%, 0.5%, 1.0%,

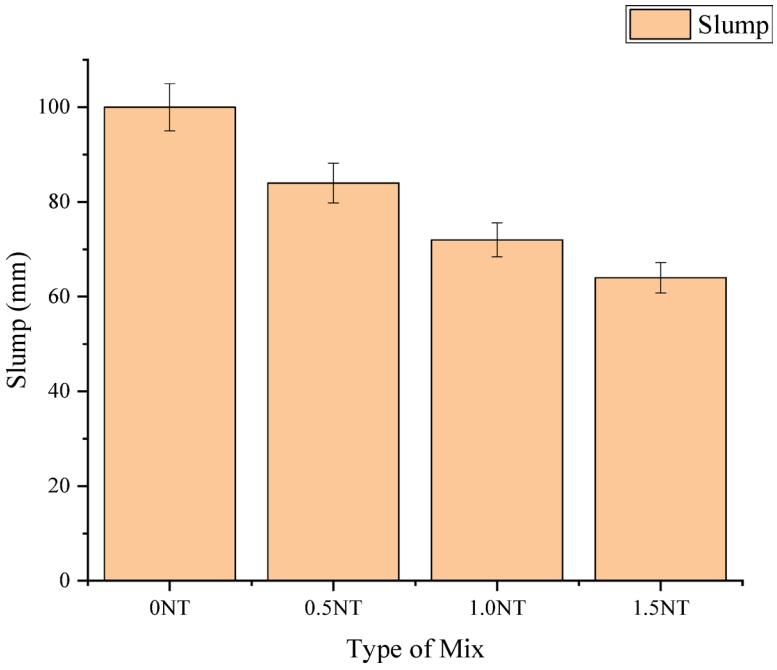


**Fig. 17**. The slump value of different mix prepared.

| Cube designation | 7 days (MPa) | Increase in CS (%) | 28 days (MPa) | Increase in CS (%) | 90 days (MPa) | Increase in CS (%) | 180 days (MPa) | Increase in CS (%) |
|---|---|---|---|---|---|---|---|---|
| 0NT | 32.50 ± 1.20 | – | 50.66 ± 1.05 | -- | 55.10 ± 0.98 | – | 58.20 ± 1.12 | – |
| 0.5NT | 36.10 ± 0.95 | 11.07 | 56.00 ± 1.10 | 10.54 | 62.40 ± 1.25 | 13.24 | 64.50 ± 1.08 | 10.82 |
| 1NT | 40.55 ± 1.30 | 24.76 | 61.80 ± 1.15 | 21.98 | 68.20 ± 1.05 | 23.77 | 71.00 ± 1.22 | 21.99 |
| 1.5NT | 43.90 ± 1.25 | 35.07 | 65.20 ± 1.03 | 28.70 | 72.25 ± 1.18 | 31.12 | 75.25 ± 1.10 | 29.29 |

**Table 5**. CS of NT-incorporated GPC.

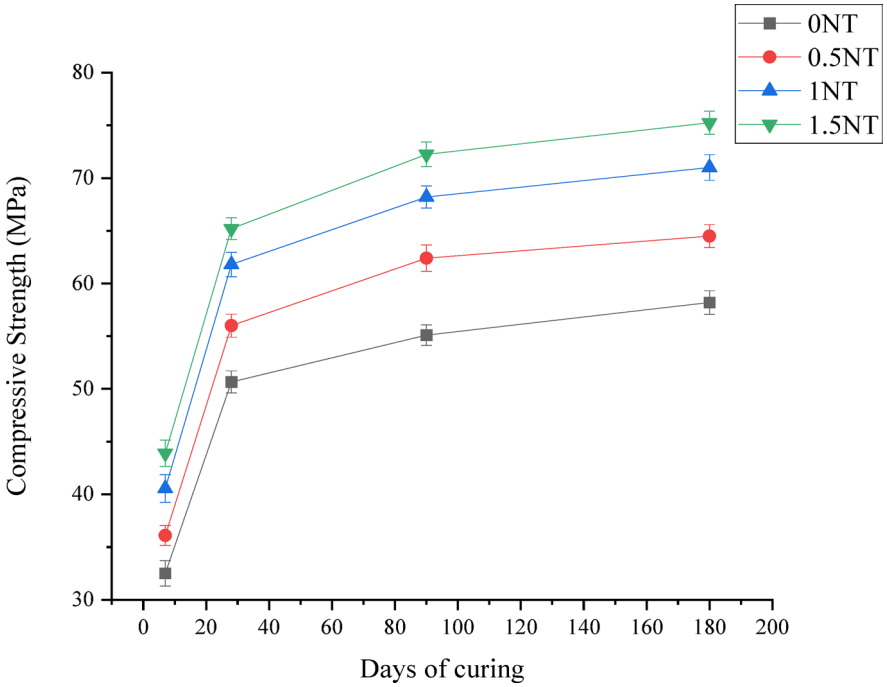


**Fig. 18**. CS of different mix prepared.

and 1.5% NT mixes, respectively. The rise in strength over time can be attributed to the role of nanoparticles in enhancing the bonding between the matrix ingredients, which in turn improves the impermeability and overall strength of the concrete. These results indicate that the addition of NT significantly enhances the strength properties of M40 grade concrete, transforming it into a higher strength concrete capable of performing better under various load conditions. The comparison of the CS at varying percentage of NT is visually presented in Fig. 18.

The significant increase in the percentage of gain in strength is also observed by other researchers after the incorporation of 1.5% NT in concrete due to the participation of NT in pozzolanic reaction, which is helpful in accelerating the phenomena of development of C-S-H gel[19,26,49]. In another study conducted by Mousavi, et al.[50]. The optimal NT percentage was found to be between 1% and 2%. The CS of NT based concrete is decreased after the incorporation of an excess amount of NT due to the non-uniform dispersion of NT particles in the matrix[51].

## Split tensile strength (STS)

As presented in Table 6, the results are reported as mean ± SD, $n = 3$ for each mix. The STS exhibited a clear positive correlation with the increasing dosage of NT. The maximum rise in STS was observed in the mix containing 1.5% NT, which showed an impressive 30.30% improvement in tensile strength at 28 days compared to the 0NT. Concrete mixes with 0.5% NT and 1.0% NT also exhibited increases in STS of 6.81% and 16.28%, respectively. The observed gain in tensile strength can be attributed to the role of nanoparticles, which enhance the fracture resistance of the concrete matrix.

The nanoparticles improve the overall structural integrity by effectively controlling microcracks within the matrix at the nano-scale, leading to enhanced tensile properties (see Fig. 19). This finding aligns with the work of Jenima et al. and Zhang et al., who reported similar improvements in the tensile behavior of concrete upon incorporating nanoparticles[19,49]. A similar increase in the STS of concrete after the incorporation of NT in concrete is observed due to the promotion of pozzolanic reaction and availability of more calcium hydroxide after the incorporation of 1.5% NT[52].

| Cylinder designation | 28 days (MPa) | Increase in STS (%) |
|---|---|---|
| 0NT | 2.64 ± 0.132 | -- |
| 0.5NT | 2.82 ± 0.141 | 6.81 |
| 1NT | 3.07 ± 0.153 | 16.28 |
| 1.5NT | 3.44 ± 0.17 | 30.30 |

**Table 6**. STS of NT-incorporated concrete mix.

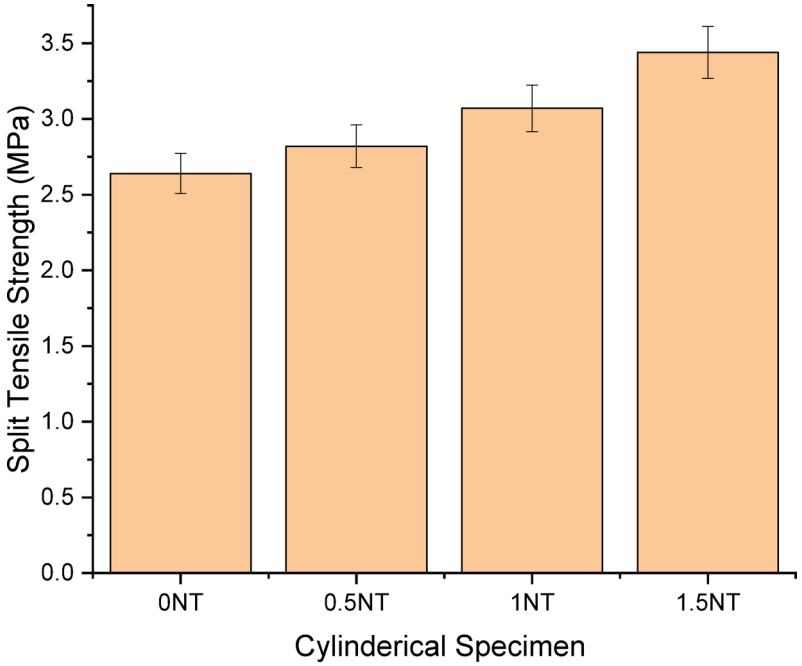


**Fig. 19**. STS of NT incorporated concrete mix.

## Flexural strength (FS)

Optimizing mix design, selecting suitable additives, and carefully choosing materials are essential for enhancing the FS of NT-incorporated composites, similar to their role in improving CS. This improvement strengthens the concrete's resistance to bending and cracking, ultimately enhancing its durability and toughness[5]. As illustrated in Table 7, results are reported as mean ± SD, $n = 3$ for each mix. The FS of concrete showed a significant increase with the incorporation of NT. The highest improvement, 40.74%, was observed in the 1.5% NT-based concrete beams after 28 days of curing, compared to the 0NT.

Concrete mixes with 0.5% NT and 1.0% NT exhibited increases of 3.70% and 25.92%, respectively. Notably, the experimentally determined FS was found to be higher than the values predicted by the guidelines in IS 456–2000 [34], indicating the improvement in the working of the nanoparticle-modified concrete. This trend indicates that the IS 456 code is conservative for the concrete mixes incorporating NT. While such conservatism ensures safety in structural design, it may underestimate the actual flexural capacity of NT-modified concretes. For member design, this implies that IS 456-based predictions will likely lead to higher safety margins when NT is used. However, in serviceability checks (e.g., deflection and cracking), underestimating the flexural strength could result in more restrictive design outcomes than what the material can actually sustain. Therefore, the findings suggest that while the current IS 456 expression remains safe, refinement of code equations may be required to better capture the contribution of nano-modified concretes, particularly when optimizing for performance and economy. A visual comparison of the FS values is presented in Fig. 20. The observed gain in FS can be attributed to the role of nanoparticles in improving the compaction and concrete densification. Furthermore, nanoparticles contribute to improved fracture resistance by controlling the propagation of microcracks at the nano-scale, thereby strengthening the matrix and resulting in better overall flexural performance.

## Rebound hammer (RH) test

A RH test was performed to check the penetration resistance and quality of concrete before the CS test. The different readings of RN on each surface of the cube were witnessed and presented in Table 8. The average readings of RN on concrete cube surfaces validate the standard CS test performed in CTM. The UPV test results, presented in Table 9, indicate a notable trend in the behavior of concrete incorporated with varying dosages of

| Beam designation | 28 days (MPa) | Increase in FS (%) | $F_{cr}$ = 0.7√fck (Mpa) | 90 days (MPa) | Increase in FS (%) |
|---|---|---|---|---|---|
| 0NT | 6.75 ± 0.337 | – | 4.97 | 7.5 ± 0.375 | – |
| 0.5NT | 7.0 ± 0.35 | 3.70 | 5.23 | 8.0 ± 0.4 | 6.66 |
| 1NT | 8.5 ± 0.425 | 25.92 | 5.50 | 9.0 ± 0.45 | 20 |
| 1.5NT | 9.5 ± 0.47 | 40.74 | 5.65 | 10.5 ± 0.525 | 40 |

**Table 7**. FS of NT-incorporated concrete mix.

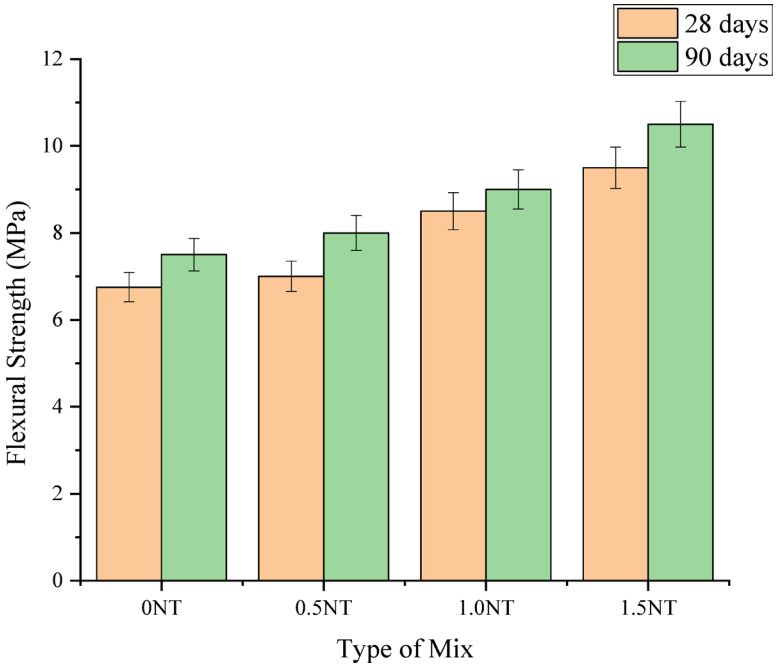


**Fig. 20**. Flexural strength of NT incorporated concrete mix.

| Cube designation | RN | CS (MPa) via RN | CS (MPa) experimental | Variation % in RN CS vs. experimental CS (± 25%) as per IS 13,311 Part 2-1992 (reaffirmed in 2004) |
|---|---|---|---|---|
| 0NT | 46 | 41.00 | 50.35 | 18.57 |
| 0.5NT | 51 | 44.00 | 54.70 | 19.56 |
| 1NT | 52 | 51.00 | 62.00 | 17.74 |
| 1.5NT | 54 | 60.00 | 65.30 | 8.11 |

**Table 8**. NT-based concrete's RN vs. experimental CS test results.

NT. It was observed that the UPV values increased as the NT dosage was enhanced, reaching the highest values at a 1.5% NT dosage. This trend was consistent across all curing periods.

The improvement in UPV with increasing NT content suggests enhanced homogeneity and compaction of the concrete matrix, which is reflective of the nanoparticles strengthening the internal structure of the concrete and improving the transmission of ultrasonic waves. The calibration data for the RN to CS conversion exhibit a strong correlation, with a coefficient of determination ($R^2$) of 0.856 (refer to Fig. S2 in the Supplementary Materials).

## Ultrasonic pulse velocity (UPV) test

The different values of UPV observed for each mix are presented in Table 9. The UPV of the conventional concrete is 4.27 km/s, while NT incorporated concrete mixes range from 4.50 to 4.55 km/s UPV. Initially, UPV decreases with the addition of 0.5% NT nanoparticles, but subsequently increases as the NT% increases, following the guidelines of IS 13,311 Part 1-1992 (reaffirmed in 2004)[43]. This increase in UPV is attributed to the NT nanoparticles filling the concrete's pores, resulting in a denser matrix. The denser structure reduces the

| Cube designation | UPV (km/sec) | CS (MPa) experimental | % increase in CS | Concrete quality |
|---|---|---|---|---|
| 0NT | 4.27 | 50.35 | – | Good |
| 0.5NT | 4.22 | 54.7 | 15.05 | Good |
| 1NT | 4.50 | 62 | 25.38 | Excellent |
| 1.5NT | 4.55 | 65.3 | 35.05 | Excellent |

**Table 9**. NT-based concrete's UPV value vs. experimental compressive strength test results.

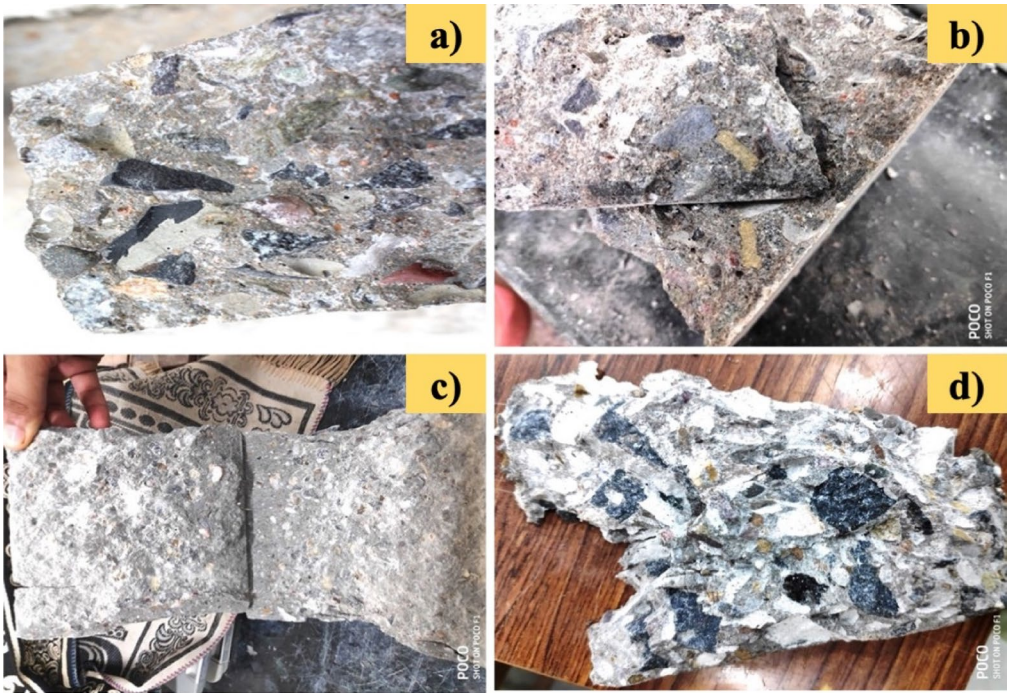


**Fig. 21**. Mode of failure of concrete cube specimen (**a**) 0NT, (**b**) 0.5NT, (**c**) 1.0NT, and (**d**) 1.5NT.

travel time of ultrasonic pulses through the concrete, thereby increasing pulse velocity. The findings established a highly reliable correlation between UPV and CS, achieving a calibration with a coefficient of determination ($R^2$) of 0.998 (refer to Fig. S1 in the Supplementary Materials).

## Cracking pattern and mode of failure

The cracking pattern and mode of failure of NT-based concrete were observed. In NT based M40 grade concrete, incorporating NT made the concrete more robust. Hence, both modes of failure mentioned above coincide in equal amounts, making the concrete high-strength concrete. The aggregate failure occurred when nano cement was used in mortar paste, as shown in Fig. 21a. M40 grade concrete was used in both cases to understand the bond and aggregate failure. Figure 21b–d show that both bond and aggregate failure simultaneously occurred in the concrete cubes of 0.5NT, 1NT, and 1.5NT equally. In addition, the concrete beams with NT in the mix show a narrow and zigzag crack pattern, compared to straight and broader cracks in the conventional concrete beams.

## Petrographic studies on cement mortar matrix

To better understand the Petrographic Studies of cement mortar cubes containing nanomaterials, it is better to understand the structure of NT at a microscopic level in microstructure characterization using a microscope. The microscopic structure of normal mix and NT-based cement mortar paste with 0%, 0.5%, 1%, and 1.5% doses was studied with a microscope, and results are shown in Figs. 22a–b and 23a–f under ordinary and polarized light. Only the Photomicrograph of 0NT exhibits tiny air-entrapped pores within the cement mortar paste matrix compared to 0.5NT, 1.0NT, and 1.5NT.

## Petrographic studies of concrete cubes

The petrographic study of the NT-based concrete matrix was conducted. The microscopic structure of the NT-based concrete matrix with 0.0%, 0.5%, 1%, and 1.5% dosage is presented in Fig. 24a–f under ordinary and polarized light. The micropores are clearly visible in 0.5% NT incorporated concrete matrix, which is reduced after further increment in the dosage of NT in concrete, as shown in Fig. 24a–f. The contact with aggregate grains becomes dense after incorporating NT in the concrete matrix.

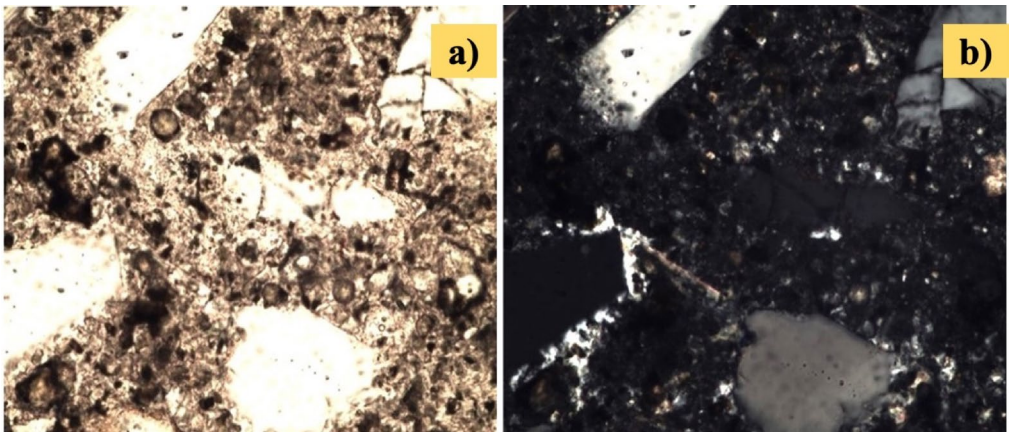


**Fig. 22**. Cement mortar picture of 0NT in (**a**) ordinary and (**b**) polarized light.

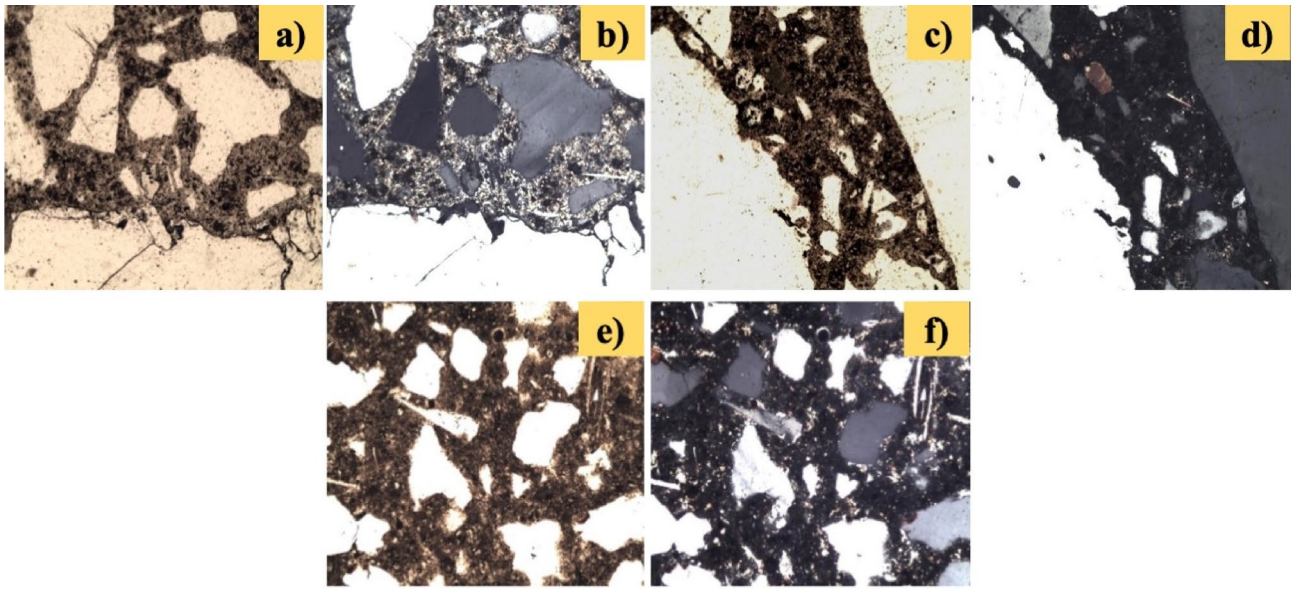


**Fig. 23**. Cement mortar picture of: (**a**) ordinary and (**b**) polarized light for 0.5NT, (**c**) ordinary and (**d**) polarized light for 1.0NT, (**e**) ordinary and (**f**) polarized light for 1.5NT.

The enhancement in the densification of the concrete matrix results in a reduction in the pores, improvement in the reduced pores, and improved strength. This is clearly evident in the petrographic studies of the concrete mix. This direct relation between the microstructure and strength of the concrete matrix is also observed by many researchers, where the microstructure improvement is observed after the incorporation of nanoparticles in the cement and concrete matrix[19,49,53,54].

## SEM analysis

Figures 25a–d and 26a–d represent the SEM images of concrete matrix. Coarse aggregate looks shiny and smooth, while the cement mortar matrix shows a rough and dull texture. The images taken were focused only on the concrete mortar matrix and coarse aggregate interface in SEM analysis. From the other perspective, the focus was only on the bond of the concrete mortar matrix with coarse aggregate. Hence, the SEM images of NT-based concrete are presented below in Figs. 25a–d and 26a–d. SEM images were taken at two magnifications, i.e., 65x and 500x.

The availability of the wide pores in the matrix without NT shown in Fig. 25a–b shows that concrete is less durable without NT, but in the NT incorporated matrix, the pores are much less and have better microstructure due to pore and voids filling capacity. The absence of hydration and C-S-H gel in Fig. 25a–b shows the weakening in the mechanical properties, but in the NT incorporated matrix, CH crystals are fully consumed and produce large quantities of C-S-H gel and develop a dense concrete[19,49]. The incorporation of NT contributes to a denser microstructure by effectively filling micro- and nanoscale cracks and pores, thereby enhancing the overall compactness and microstructure of the concrete[55].

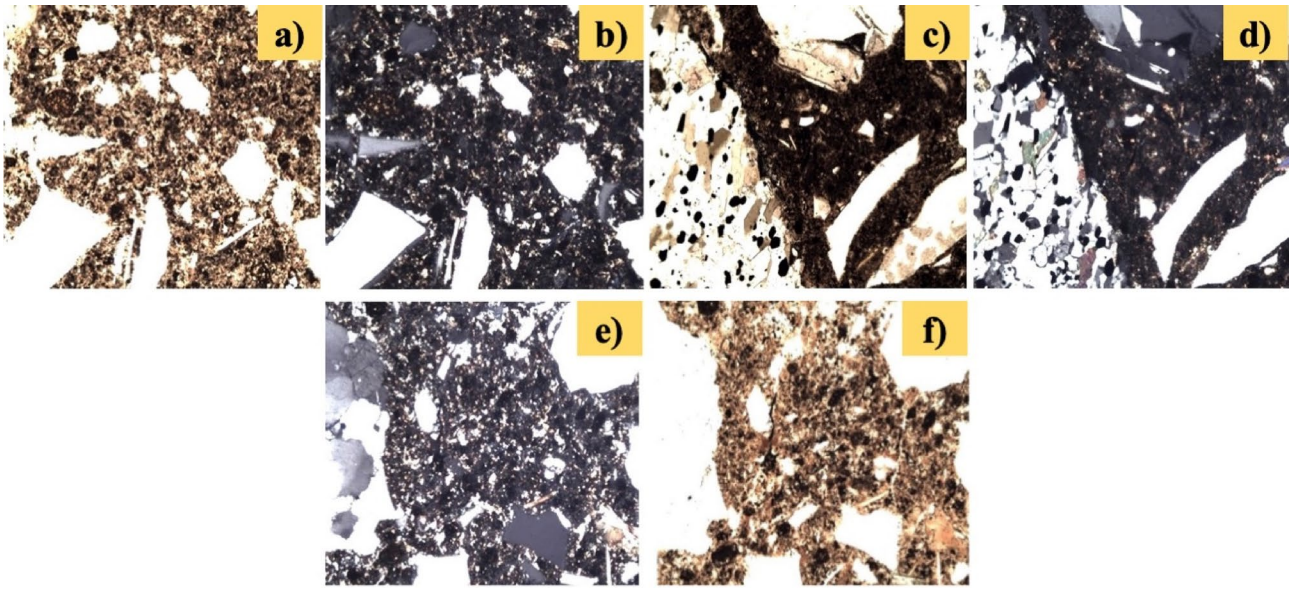


**Fig. 24**. Concrete matrix picture of: (**a**) ordinary and (**b**) polarized light for 0.5NT, (**c**) ordinary and (**d**) polarized light for 1.0NT, (**e**) ordinary and (**f**) polarized light for 1.5NT.

Moreover, findings of this study indicate that the incorporation of NT significantly influences the hydration mechanisms of cementitious systems. Specifically, NT was observed to enhance the $C_3S$ and $C_2S$ hydration, accelerating the formation of CH as shown in Figs. 25c–d and 26a–d. This augmentation in CH concentration suggests that NT plays a dual role—both as a hydration promoter and a nucleation site for CH crystallization. While this phenomenon contributes to early-age strength development, excessive CH formation may also alter the long-term microstructural stability of the cement matrix. These results align with previous research[5], which has demonstrated that NT modifies hydration kinetics by providing additional nucleation to polarize and form the gel, leading to a denser and more refined pore structure. This finding aligns with a similar observation noted by Ghanim et al.[56].

## Synergetic mechanism of NT on concrete

The inclusion of NT into concrete matrices introduces a synergetic mechanism that enhances both the microstructural integrity and the long-term performance of cementitious composites (see Fig. 27). At the nanoscale, titanium dioxide particles contribute to the hydration process by acting as nucleation sites, accelerating the transformation of $C_3S$ and $C_2S$ into C-S-H gel. This accelerated hydration (nucleation effect) leads to a denser microstructure, which directly enhances the early-age strength of concrete. Furthermore, NT exhibits pozzolanic reactivity, particularly in the highly alkaline environment of cement paste, where it reacts with the CH released during hydration to produce additional C-S-H gel. This reaction not only densifies the ITZ between aggregates and paste but also reduces the availability of free CH, thereby improving durability. Physically, the ultrafine NT particles fill micro-voids and capillary pores, refining the pore structure and reducing permeability. In combination, these chemical and physical mechanisms produce a synergistic enhancement of mechanical properties, durability, and resistance to aggressive environments, positioning nano titanium as a multifunctional nanomaterial in advanced concrete technology. These mechanisms together result in a more compact and resilient microstructure, even in the absence of traditional pozzolanic additives.

## Durability analysis under harsh environments

*Durability test: concrete exposure to harmful chemicals*

The CS results of NT-based concrete exposed to harmful chemicals is shown in Fig. 28. During the exposure to 4% HCl-Water solution, CS is increased by 5.93%, 17.70%, and 28.72% after incorporating 0.5%, 1% and 1.5% NT in comparison with 0% NT concrete. After exposure to 4% HCl, the highest CS of 51.40 MPa is achieved after incorporating a 1.5% dosage of NT. During exposure to 4% $H_2SO_4$, CS of NT based concrete is increased by 15.35%, 30.28%, and 42.94% after incorporating 0.5%, 1% and 1.5% NT in comparison with 0% NT concrete. The observed improvement in the strength retention of NT-incorporated concretes after acid exposure can be attributed to both physical and chemical mechanisms. The high surface area and photocatalytic reactivity of NT promote additional nucleation sites during hydration, leading to the formation of a denser C–S–H gel matrix. This refinement of pore structure reduces the ingress of aggressive ions, thereby delaying the leaching of $Ca(OH)_2$ and decalcification of C–S–H under acidic environments.

Microstructural analyses support this interpretation: XRD patterns of NT mixes show reduced intensity of portlandite peaks and enhanced amorphous humps associated with C–S–H, indicating consumption of $Ca(OH)_2$ and densification of hydration products. EDS spectra further reveal lower Ca/Si ratios in acid-exposed NT concretes compared to control specimens, signifying stabilization of C–S–H and reduced susceptibility

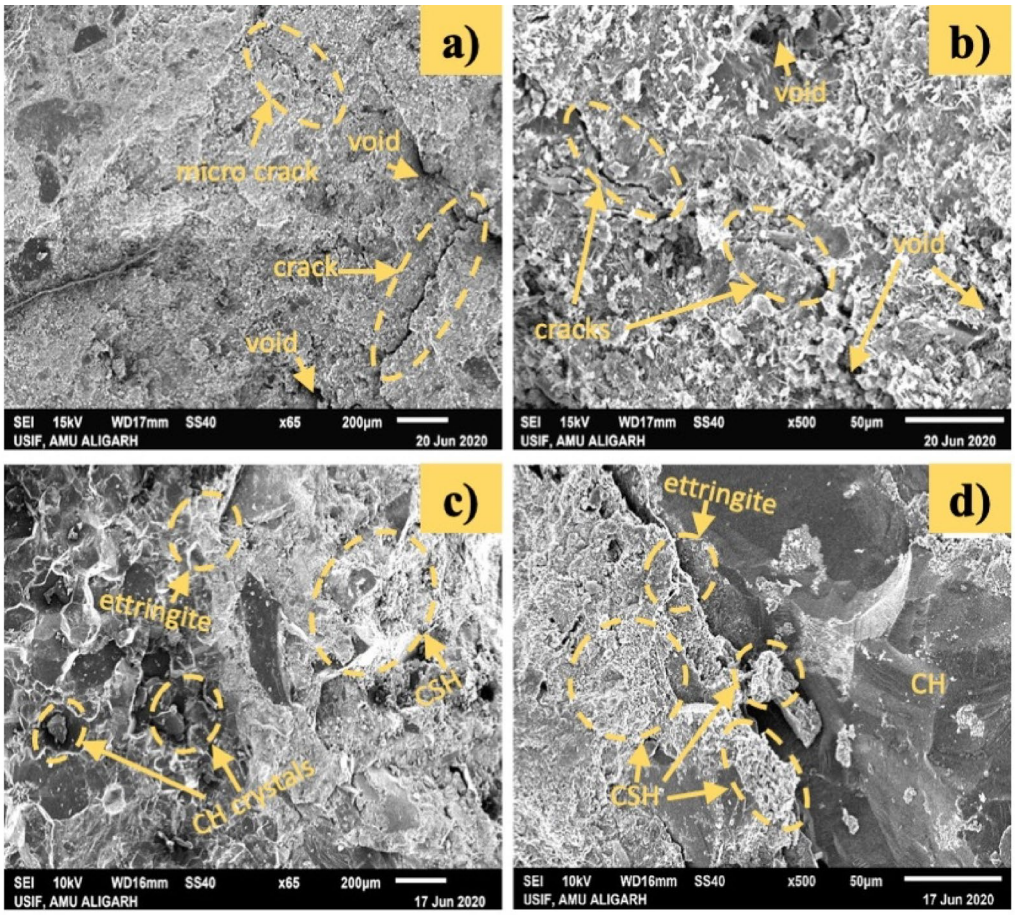


**Fig. 25**. Interface SEM images of NT based concrete: (**a**) 0NT at 200 µm, (**b**) 0NT at 50 µm, (**c**) 0.5NT at 200 µm, (**d**) 0.5NT at 50 µm.

to acid dissolution. These microstructural features explain why NT concretes retained a higher proportion of compressive and tensile strength after sulfuric acid exposure. Thus, the incorporation of NT not only enhances early hydration but also imparts long-term durability benefits by mitigating acid-induced degradation.

In addition to compressive strength testing, the durability of the specimens was further evaluated through mass loss measurements and observations of surface condition. Each specimen was oven-dried to a constant mass before immersion and reweighed after 90 days of exposure to 4% NaCl, HCl, and $H_2SO_4$ solutions.

The percentage mass change was calculated relative to the initial dry mass. Results of variation in the mass due to chemical exposure are presented in Table 10. The data reveal that NT-incorporated concretes exhibited substantially reduced mass loss under all aggressive exposures compared to the control (0NT). After 90 days of immersion in $H_2SO_4$, the 0NT specimens lost 6.4% of their initial mass, whereas the 1.5NT mix lost only 2.9%. A similar trend was noted in HCl, with 0NT losing 3.2% mass, while 1.5NT lost just 1.8%. In NaCl solution, negligible mass loss (< 1%) was recorded across all mixes, but the control specimens showed surface efflorescence and minor scaling, while NT mixes maintained intact surfaces. Figure 29 shows the visual condition of concrete specimens after 90 days of exposure to harmful chemicals. Surface scaling observations aligned with mass loss trends. The 0NT specimens exposed to acid solutions showed severe surface softening, spalling, and visible roughness, whereas NT concretes exhibited only minor surface changes, with denser and smoother surfaces. Under NaCl exposure, 0NT specimens developed whitish deposits and fine cracks, while NT mixes remained largely unaffected.

*Durability test: concrete exposure to alternate Freeze-Thaw*

The long-term serviceability of structures in cold regions is analysed by free-thaw resistance. The CS result of the NT-based concrete under freeze-thaw conditions is shown in Table 11. The result shows the positive impact of the incorporation of NT on the strength of concrete exposed to freeze-thaw conditions (limited range of freeze/thaw cycles, up to 120 cycles), which aligns with Tanimola and Efe findings[49]. The maximum increment in the strength up to 17.93% is observed after incorporating 1.5% NT in concrete. However, only a minor improvement in the strength was observed after the inclusion of 1% NT in concrete. The pore-filling capacity of NT helps in reducing the pores, ultimately reducing the place of water to freeze, increasing the strength. The freeze-thaw damage to the concrete is due to the uneven expansion between the aggregate and the concrete matrix[57]. As the expansion coefficient is directly proportional to the humidity of the material. However, the early age hydration

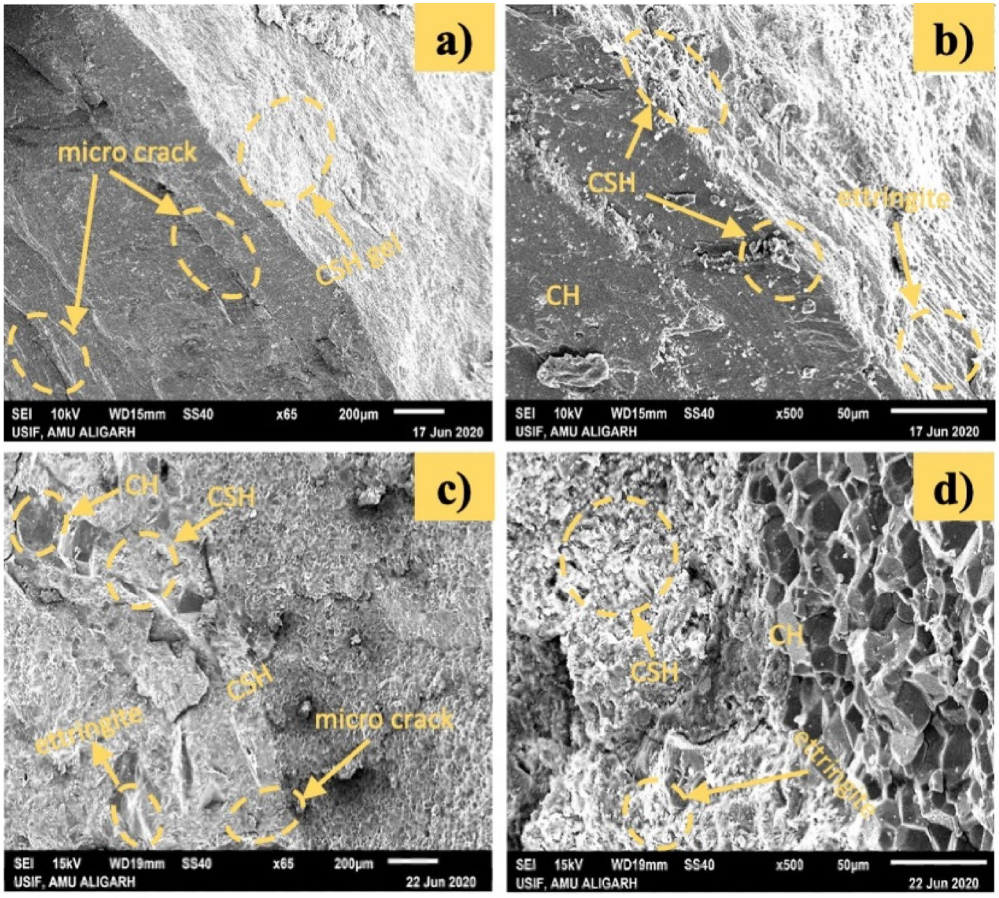


**Fig. 26**. Interface SEM images of NT based concrete: (**a**) 1.0NT at 200 µm, (**b**) 1.0NT at 50 µm, (**c**) 1.5NT at 200 µm, (**d**) 1.5NT at 50 µm.

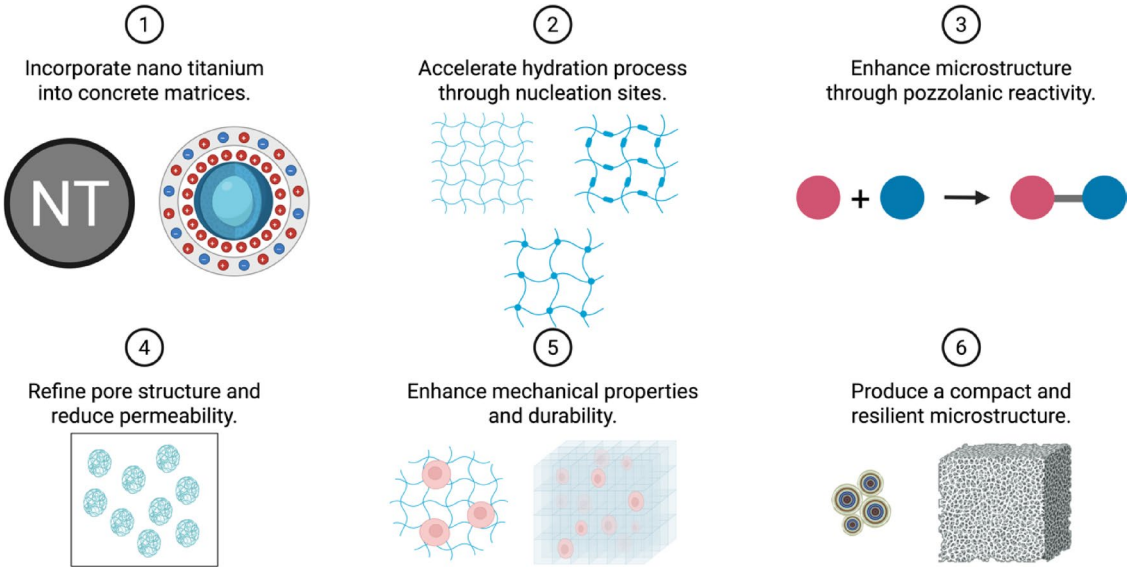


**Fig. 27**. Synergetic mechanism.

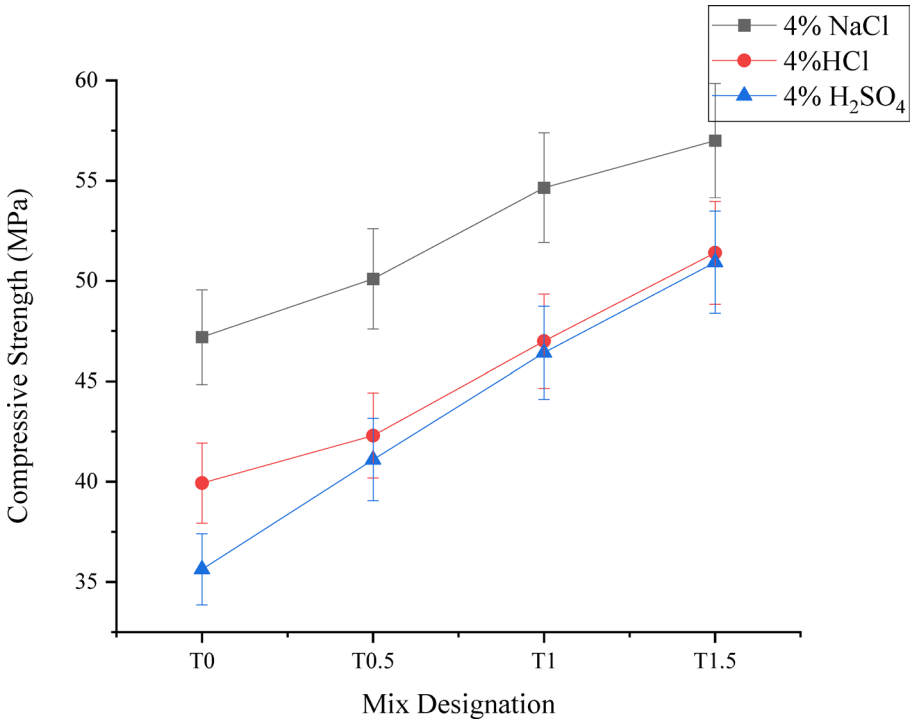


**Fig. 28**. CS of NT based concrete exposed to harmful chemicals.

| Mix | Mass gain in 4% NaCl (%) | Mass loss in 4% HCl (%) | Mass loss in 4% $H_2SO_4$ (%) | Surface scaling/appearance |
|---|---|---|---|---|
| 0NT | 0.3 | 3.2 | 6.4 | Severe scaling and spalling in acid; efflorescence & fine cracks in NaCl |
| 0.5NT | 0.2 | 2.5 | 4.8 | Moderate surface scaling in acid; minor whitish deposits in NaCl |
| 1NT | 0.1 | 2.0 | 3.6 | Slight roughness in acid; surface intact under NaCl |
| 1.5NT | 0.0 | 1.8 | 2.9 | Smooth surface, negligible scaling; no efflorescence under NaCl |

**Table 10**. Results of variation of mass due to chemical exposure.

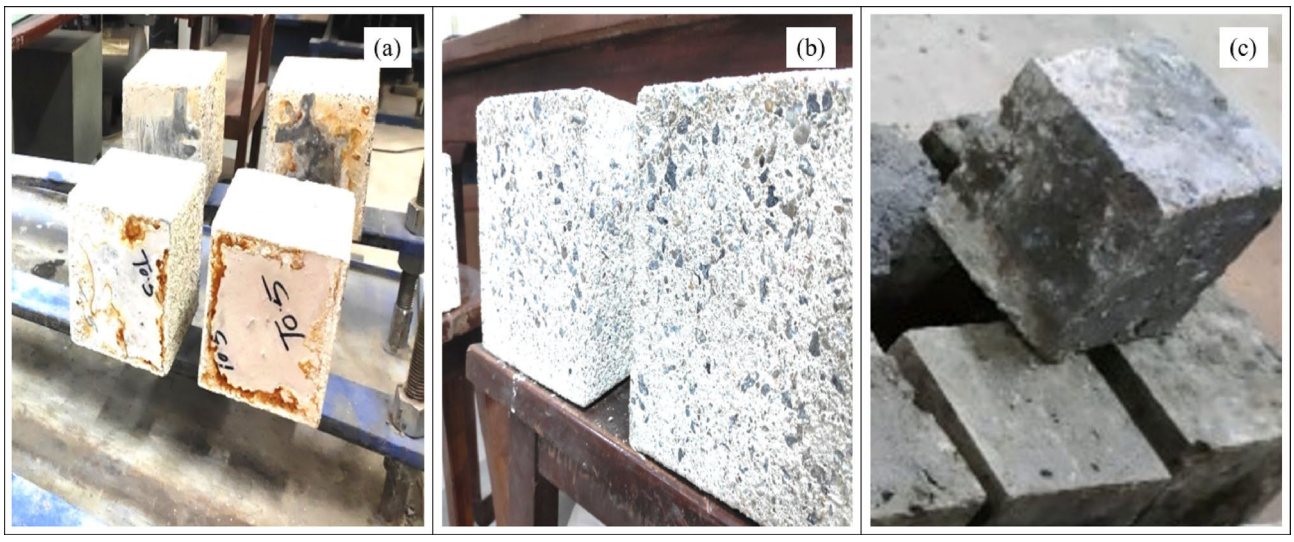


**Fig. 29**. Visual condition of concrete specimens after 90 days of exposure to (**a**) 4% HCl, (**b**) 4% $H_2SO_4$, and (**c**) 4% NaCl.

| Cube designation | Compressive strength (MPa) | % Increase in compressive strength |
|---|---|---|
| 0NT | 56.15 | – |
| 0.5NT | 59.28 | 5.57 |
| 1NT | 63.82 | 13.65 |
| 1.5NT | 66.22 | 17.93 |

**Table 11**. Test results of NT-based concrete's compressive strength after exposure to freeze-thaw process up to 120 cycles.

| Mix | Mass loss (%) | RDME (%) | VDI (0–3) | CS loss per cycle (%) |
|---|---|---|---|---|
| 0NT | 2.5 | 82 | 3 | 0.17 |
| 0.5NT | 1.8 | 88 | 2 | 0.12 |
| 1NT | 1.2 | 93 | 1 | 0.07 |
| 1.5NT | 0.8 | 95 | 0 | 0.05 |

**Table 12**. Freeze-thaw durability indicators.

| Cube designation | Carbonation depth (mm) at the duration of 30 days |
|---|---|
| 0NT | 1.4 ± 0.2 |
| 0.5NT | No carbonation observed |
| 1NT | No carbonation observed |
| 1.5NT | No carbonation observed |

**Table 13**. Test results NT-based concrete's carbonation depth.

is accelerated by the NT incorporated, but NT has no significant impact on the hydration process at a later age. The cracks formed during the freeze-thaw cycles are filled by the NT incorporated, improving the strength of concrete by bridging the gap between nano and microcracks.

The extended freeze–thaw durability indicators (Table 12) show that NT significantly enhances resistance to cyclic deterioration. The mass loss of the control mix (0NT) was 2.5% after 120 cycles, accompanied by severe scaling (VDI = 3), while 1.5NT specimens lost only 0.8% mass and remained intact (VDI = 0). The relative dynamic modulus decreased to 82% in the control mix, compared to 95% in 1.5NT concrete, confirming reduced microcracking and stiffness degradation. Similarly, compressive strength loss per cycle dropped from 0.17% (0NT) to 0.05% (1.5NT).

*Durability test: accelerated carbonation test*

The result of the carbonation test of concrete with and without NT is shown in Table 13. The control specimens (0NT) exhibited an average carbonation depth of 1.4 ± 0.2 mm, whereas all NT-incorporated mixes (0.5NT, 1NT, 1.5NT) showed no measurable carbonation depth within the 1 mm powder increment resolution. This is due to the reduction of the pores and the elimination of the passage of carbon by incorporating the nanomaterial in concrete. The dense concrete after incorporation of NT does not become the reason for exposure of the interior layer of concrete to deterioration due to carbon. These findings of negligible carbonation in NT-incorporated specimens after 30 days of exposure are consistent with recent literature. Wan et al. (2019) reported that even at 28 days of accelerated carbonation, concretes with nano-silica showed markedly lower carbonation depths compared to control mixes[58]. Similarly, Snehal et al. (2023) observed that mortars with nano-silica exhibited delayed carbonation kinetics under high $CO_2$ exposure due to microstructural densification and reduced capillary porosity[59]. Moreover, a recent review on titanium dioxide nanoparticles in cementitious composites noted that increasing NT dosage tends to reduce carbonation penetration (especially at early ages), which is attributed to pore refinement and improved hydration product stability[19]. Thus, our results showing "no measurable carbonation" in NT mixes after 30 days align with the mechanism that nanoparticle additions refine the microstructure and limit $CO_2$ diffusion in the short term.

*Durability test: surface electrical resistivity test*

The electrical resistivity increases with an increment in the dosage of incorporation of NT in concrete, as shown in Table 14. It was noticed that a maximum resistance of 46.50 kilo ohm-cm is observed after the incorporation of 1.5% NT in concrete. Table 14 also shows the penetrability of chloride ions in concrete conforming to the guidelines given in AASHTO TP 95[45]. It was noticed that the penetration of chloride ions in conventional concrete was low. However, the penetrability of chloride ions was very low after incorporating NT in concrete.

| Cube designation | Resistivity (kilo ohm-cm) | Chloride ion penetrability | Chloride ion penetrability (according to AASHTO TP 95) (kilo ohm-cm) [45] |
|---|---|---|---|
| 0NT | 33.80 | Low | High < 12 |
| 0.5NT | 36.80 | Low | Low- 21 to 37 |
| 1NT | 42.90 | Very Low | Very Low- 37 to 254 |
| 1.5NT | 46.50 | Very Low | Negligible- >254 |

**Table 14**. Test results of NT-based concrete's chloride ion penetrability.

| Cube designation | RCPT Coulombs (Q) | Chloride ion penetrability | Chloride ion penetrability (According to ASTM C1202) (Q) [47] |
|---|---|---|---|
| 0NT | 2632 ± 105 | Moderate | High: >4000<br>Moderate: 2000–4000<br>Low: 1000–2000<br>Very Low: 100–1000<br>Negligible: < 100 |
| 0.5NT | 2759 ± 112 | Moderate | |
| 1NT | 3200 ± 128 | Moderate | |
| 1.5NT | 3540 ± 135 | Moderate | |

**Table 15**. NT-based concrete's chloride ion penetrability test result.

*Durability test: rapid chloride penetration test (RCPT)*

Chloride ion penetrability of the concrete with and without NT was observed, and the results are shown in Table 15. The concrete with NT incorporation gives moderate penetrability with the value of charge 2759 ± 112 coulombs, 3200 ± 128 coulombs, and 3540 ± 135 coulombs with the incorporation of 0.5%, 1%, and 1.5% NT dosage as per the guidelines given in ASTM C1202[47]. The NT contributes well in reducing the penetration of chloride due to high fineness and pore-filling capacity. The decrease in penetrability after the incorporation of NT is also due to the decrease in porosity and more refinement of the structure. Rawat et al.[55] investigated the influence of NT on chloride penetration in concrete and observed that its presence significantly enhances resistance against chloride ingress. This improvement is attributed to nano NT's role in hydration, which promotes the formation of a compacted and dense microstructure. As a result, the refined pore structure helps mitigate the effects of aggressive environments. However, excessive incorporation of nano NT can be detrimental to durability, as reduced spacing between nanoparticles and a decline in calcium hydroxide content may hinder the formation of a well-structured strengthening gel, ultimately compromising the compactness of the matrix.

In contrast, resistivity values increased with NT dosage. This apparent contradiction arises from the different sensitivities of the two methods: RCPT is strongly influenced by pore solution conductivity, whereas surface resistivity primarily reflects pore structure refinement. Incorporation of NT refines pore size distribution (confirmed by SEM and petrography) and thus raises resistivity. At the same time, NT accelerates hydration and increases ionic species ($Ca^{2+}$, $OH^{-}$) in the pore solution, elevating conductivity and leading to higher RCPT values. Similar trends have been reported by another study[55]. Direct pore solution conductivity measurements were not available in this study, but the combined results suggest that NT reduces transport pathways but increases ionic mobility, underscoring the need for multiple durability indices in nano-concrete assessment.

*Durability test: concrete exposure to oven drying at 300 °C*

The compressive strength result of the specimens exposed to oven drying at 300 °C with and without NT is shown in Table 16. It was visible that the rise in strength was due to the rise in the amount of NT in concrete. The maximum increase in the strength, i.e., 35.89% was observed after the incorporation of 1.5% NT in concrete.

The increment in the CS at elevated temperature was noticeable due to the elevated temperature being responsible for the additional hydration layer of cement product, and the other reason is the pozzolanic reactivity of the nanomaterial incorporated in concrete. The major strength component of concrete i.e. C-S-H gel is increased after incorporation of NT in concrete.

*Durability test: concrete exposure to fire at 200 °C, 400 °C, and 600 °C*

The measurement of CS at elevated temperatures is very important for analysing the performance of the structure against fire. The CS result of concrete incorporated with different dosages of NT exposed to fire at different temperatures is shown in Fig. 30. During exposure to fire at 200 °C, CS is increased by 14.90%, 24.77% and 35.48% after incorporation of 0.5%, 1%, and 1.5% NT in concrete in comparison with concrete without NT. During the exposure to fire at 400 °C, the CS is increased by 10.25%, 18.65% and 28.80% after incorporation of 0.5%, 1% and 1.5% NT in comparison with 0% NT in concrete. During the exposure to fire at 600 °C, the CS is increased by 9.17%, 6.28% and 1.00% after incorporation of 0.5%, 1% and 1.5% NT in comparison with 0% NT in concrete. From Fig. 30, it was noticed that CS is increased with the rise in the dosage of NT in concrete exposed to 200 °C and 400 °C. But a decrease in CS is observed after increasing the dosage of NT by more than 0.5% for the concrete exposed to 600 °C. CS of concrete declines with a rise in temperature of exposure for all concrete mixes.

The decrease in CS due to the rise in temperature is due to the degradation of the C-S-H gel. This is also due to the formation of gaps left behind after the elimination of the water from the mix. The binding properties of the material used get reduced due to the conversion of calcium carbonate into lime. The decrement in the

| Cube designation | CS (MPa) | % Increase in CS |
|---|---|---|
| 0NT | 44.80 | – |
| 0.5NT | 53.71 | 19.88 |
| 1NT | 57.57 | 28.50 |
| 1.5NT | 60.88 | 35.89 |

**Table 16**. Test results of NT-based concrete's CS after oven drying at 300 °C.

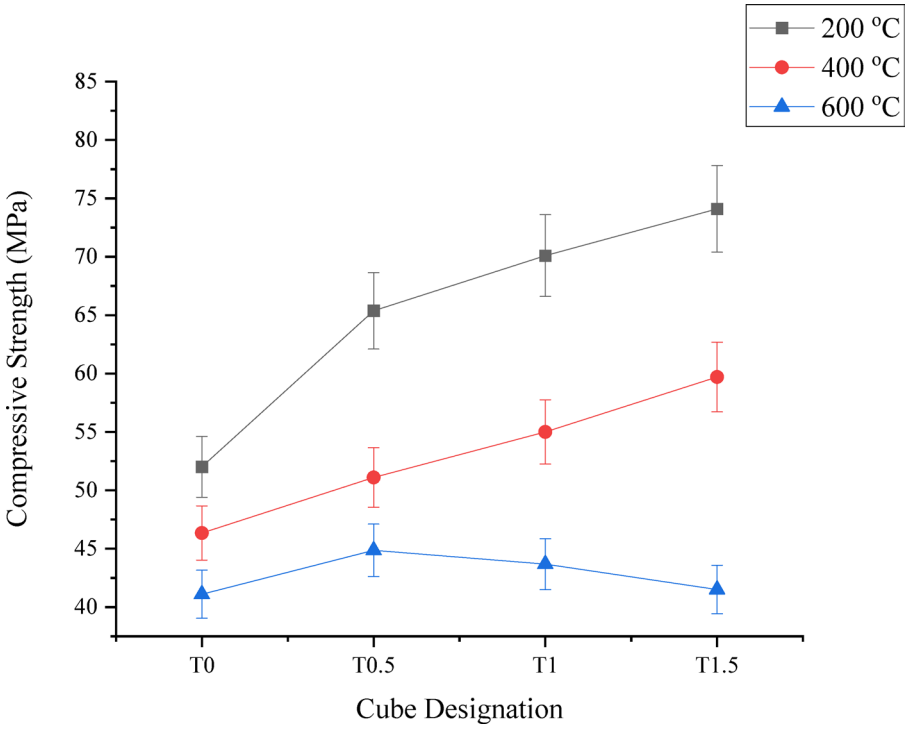


**Fig. 30**. CS of NT-based concrete exposed to fire conditions.

strength is also due to a rise in pore pressure due to temperature rise and the formation of microcracks. But in NT-incorporated concrete, the CS is not reduced much due to the filling of these micro-cracks at the nano and micro levels. Due to its ultrafine size, NT plays a crucial role in reducing porosity, thereby enhancing the overall densification of concrete and improving its resistance to high temperatures. Guler et al.[60] reported that incorporating nanoparticles led to a notable improvement in the ITZ, resulting in a more compact and dense microstructure. This enhancement contributed to the retention of compressive strength at elevated temperatures, demonstrating the effectiveness of NT in improving concrete's thermal stability.

The relatively higher strength retention of NT concretes after high-temperature exposure cannot be attributed to additional hydration, since hydration ceases and decomposition of hydration products dominates at elevated temperatures. Instead, the improvement is more plausibly explained by the microstructural densification and pore refinement imparted by NT incorporation before heating. Nanoparticles accelerate hydration at early ages, reduce porosity, and form a denser C–S–H matrix, which provides improved resistance against thermal cracking and decomposition. Several studies have reported that nanoparticles enhance pore structure refinement and improve residual strength after heating by delaying microcrack propagation[61–63]. Nevertheless, our findings are consistent with the literature evidence that NT stabilizes the microstructure before heating. This has been identified as a scope for future research, where systematic SEM/XRD analysis of NT concretes pre- and post-thermal exposure will be undertaken to confirm the underlying mechanisms.

*Durability test: capillary porosity test*

Capillary porosity test results of the NT-incorporated concrete are shown in Table 17. It was noticed that there is no significant capillary porosity in concrete with or without NT. The NT promotes hydration and densifies the structure at the nano and micro level, thereby enhancing the ITZ and controls the capillary porosity. The observed values suggest a reduced pore volume within the concrete matrix, as sorptivity is directly linked to the presence of pores. Lower sorptivity values further indicate a nonuniform pore size distribution, which can hinder water movement through the concrete. The incorporation of NT effectively fills both micro- and nanoscale pores, resulting in a denser matrix that restricts water penetration and enhances overall durability[55,60].

| Cube designation | Remarks |
|---|---|
| 0NT | Capillary porosity not observed |
| 0.5NT | Capillary porosity not observed |
| 1NT | Capillary porosity not observed |
| 1.5NT | Capillary porosity not observed |

**Table 17**. NT-based concrete's capillary porosity test results.

| Cube designation | Thickness (m) | Area ($m^2$) | Time (s) | Head (m) | Flow ($m^3$) | Permeability (k) |
|---|---|---|---|---|---|---|
| 0NT | 0.15 | 0.0225 | 86,400 | 1.5 | $5\times10^{-8}$ | $2\times10^{-10}$ |
| 0.5NT | 0.15 | 0.0225 | 86,400 | 1.5 | $1\times10^{-8}$ | $3.7\times10^{-11}$ |
| 1NT | 0.15 | 0.0225 | 86,400 | 1.5 | $1.8\times10^{-9}$ | $7.2\times10^{-12}$ |
| 1.5NT | 0.15 | 0.0225 | 86,400 | 1.5 | $1.1\times10^{-9}$ | $4.8\times10^{-12}$ |

**Table 18**. NT-based concrete's permeability test results.

The reduced sorptivity of $TiO_2$-modified concrete can be attributed to the finer particle size of $TiO_2$ and its role in enhancing C-S-H gel formation, which effectively refines the pore structure and minimizes sorptivity[8,64]. As the $TiO_2$ content increases within the C-S-H gel, sorptivity levels continue to decline. This reduction occurs due to the decreased pore interconnectivity, which subsequently limits moisture absorption. These findings are consistent with previous studies, including those reported by Rawat et al[64].

In all tested samples, the incorporation of NT as a nanomaterial in concrete resulted in a notable reduction in porosity. This decrease can be attributed to the role of NT nanoparticles as efficient fillers, gradually occupying void spaces as dispersed within the matrix. The nanoparticle clusters not only filled these spaces but also acted as nucleation sites, accelerating the hydration process. As hydration progressed rapidly within water-filled pores, overall porosity was further diminished. Research by Mohammadi et al.[65] also demonstrated a reduction in total porosity when titanium dioxide was introduced into calcium phosphate cement. Similarly, studies by Abdullah et al.[66] confirmed that substituting NT in partial replacement of Portland cement led to decreased porosity at varying concentrations, highlighting the effectiveness of NT in refining the pore structure.

*Durability test: permeability test*

The permeability test was carried out as per the guidelines given in IS 3085 – 1965[48] on concrete, and the results are shown in Table 18. It was noticed from the table that no permeability was observed in any of the mixes with or without NT. This is due to the reduction of the available pores of C-S-H. After the incorporation of NT in concrete, the elimination of these pores results in the formation of impermeable and dense structures.

At the 2-day curing mark in the study of Nazari and Riahi[26], the water absorption percentage in concrete specimens without NT (0% NT) is lower than that observed in mixes containing 1–5% NT. However, at 7 and 28 days of curing, the trend reverses, with the 1–5% NT series exhibiting reduced water absorption compared to the 0% NT specimens. This initial increase in water absorption for NT-containing mixes can be attributed to the accelerated formation of hydration products facilitated by NT nanoparticles at early curing stages. Since NT enhances the hydration process, these specimens require more water to support the formation of hydration compounds. Consequently, at the 2-day curing stage, the higher water demand in the 1–5% NT series results in greater absorption compared to the 0% NT mix. Over time, as curing progresses to 7 and 28 days, the pore structure of NT-containing concrete undergoes significant refinement, leading to decreased water permeability relative to the 0% NT specimens.

*Compressive strength test to determine modulus of elasticity (MOE) and initial tangential modulus (ITM) of concrete*

Figure 31a–c shows the stress-strain curve of concrete incorporated with different dosages of NT. The stress obtained is 58 $N/mm^2$, 62.71 $N/mm^2$, and 63.82 $N/mm^2$ with the incorporation of 0.5%, 1%, and 1.5% NT in concrete. The corresponding values of the strain are 0.0126, 0.0096, and 0.0115 obtained after incorporation of 0.5%, 1%, and 1.5% NT in concrete. Moreover, NT-based concrete's ITM and MOE values are shown in Table 19.

A significant shift in trend was observed with the incorporation of NT. Among all the tested mixtures, those containing 1.5% NT demonstrated the highest ME, which can be attributed to the nanoscale fineness of NT particles. These nanoparticles effectively fill micropores within the concrete matrix, contributing to increased stiffness. However, exceeding this optimal NT content resulted in a decline in ME. This reduction is likely due to the increased availability of $Ca(OH)_2$ crystals, which are essential for C-S-H gel formation, as well as the challenges in achieving a uniform nanoparticle distribution within the matrix. These findings align with the conclusions drawn by Rawat et al.[64] and are supported by previous research by Nazari et al.[51].

## Economic viability assessment of nano-concrete

The integration of advanced nanomaterials into concrete, while promising from a performance and durability standpoint, introduces significant complexities in cost assessment[67–70]. A comprehensive economic feasibility

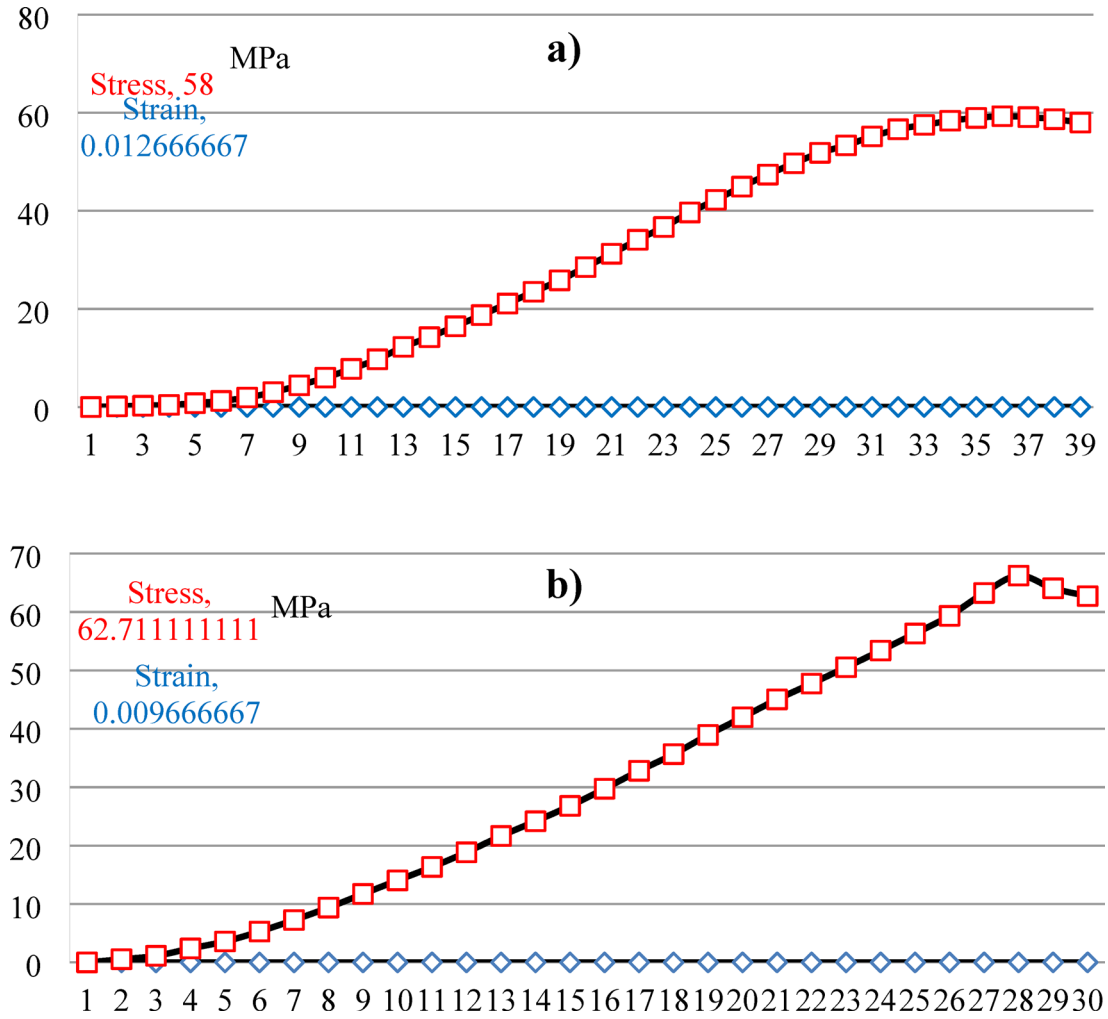


**Fig. 31**. Concrete cube specimen stress-strain curve of: (**a**) 0.5NT, (**b**) 1.0NT, (**c**) 1.5NT.

analysis must therefore extend beyond a simple comparison of initial material costs via cost-benefit analysis (CBA). While conventional OPC concrete currently holds an advantage in terms of upfront expenses, this analysis posits that the long-term economic viability of NT-concrete is potentially transformative. This section evaluates the economic implications of employing NT in concrete by comparing the direct material costs of production against the potential for long-term value generation. This value is derived from the material's enhanced mechanical properties—including CS, STS, and FS—and its superior durability performance under aggressive environmental conditions, such as exposure to harmful chemicals, freeze-thaw cycles, and reduced permeability. The cost analysis for producing one cubic meter of both conventional and NT-concrete, detailed in Table S1 (Supplementary Information), is based on prevailing material rates within the Indian market, standardized to US dollars (1 USD = 84 INR) for broader relevance. The rates of the materials used in this study are shown in Table S2 (Supplementary Information).

As provided in Table 20, the benefit cost ratio (BCR) of each mixture provides a quantitative assessment of the economic feasibility, owing to the importance of the constituent material property improvements compared to a regular concrete. These were done through a formal CBA method, which combines the calculated performance gains with the added material change cost[68,71,72]. This method does establish a concrete basis for balance assessment when considering the tradeoff between an increase in performance and the cost of sophisticated concrete.

$$\mathrm{a} = \text{Value of property (NT concrete)} \tag{6}$$

$$\mathrm{b} = \frac{\mathrm{a} - \text{Value of property (conventional concrete)}}{\text{Value of property (conventional concrete)}} \tag{7}$$

$$\mathrm{c} = \text{Value of Eq. (b)} \times \mathrm{WF} \tag{8}$$

The CBA presented on Table 20 suggests specific economic consequences of concrete mixtures with NT. Out of all the formulations analyzed, the mixture with 1.0% NT proportion had the most preferable benefit-cost ratio

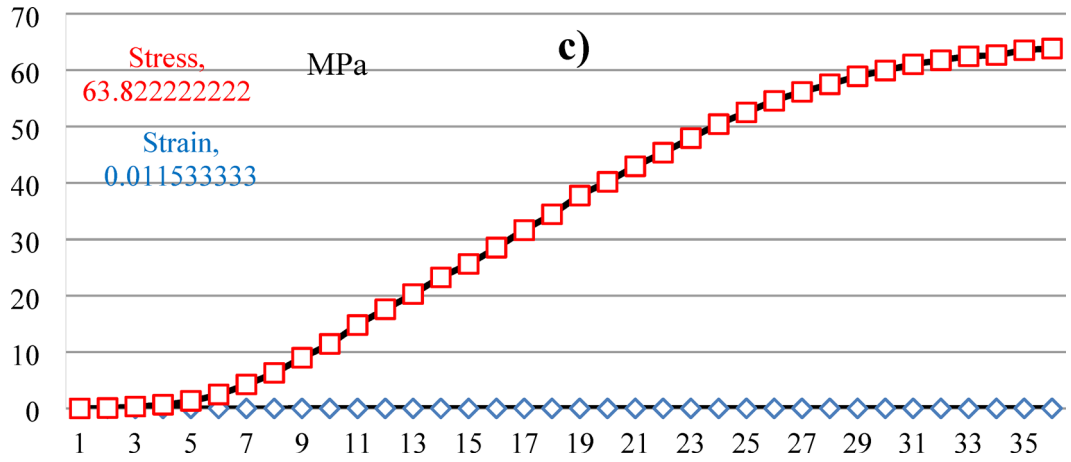


**Fig. 31.** (continued)

| Cube designation | 28 days (MPa) CS | ITM (GPa) (kN/mm²) | MOE (Ec = 5000 $\sqrt{f_{ck}}$) (GPa) (kN/mm²) IS 456: 2000 [34] | % Increase in MOE |
|---|---|---|---|---|
| T0 | 42.44 | 3.70 | 32.57 | – |
| T0.5 | 58.00 | 7.38 | 38.07 | **16.88** |
| T1 | 62.71 | 8.25 | 39.59 | **21.55** |
| T1.5 | 63.82 | 8.25 | 39.94 | **22.62** |

**Table 19**. NT- based concrete's initial tangential modulus and modulus of elasticity values.

| Property | WF | 0.5NT | | | 1.0NT | | | 1.5NT | | |
|---|---|---|---|---|---|---|---|---|---|---|
| | | a Eq. 6 | b Eq. 7 | c Eq. 8 | a Eq. 6 | b Eq. 7 | c Eq. 8 | a Eq. 6 | b Eq. 7 | c Eq. 8 |
| CS (MPa) | 10 | 56.000 | 0.105 | 1.054 | 61.800 | 0.220 | 2.199 | 65.200 | 0.287 | 2.870 |
| STS (MPa) | 10 | 2.820 | 0.068 | 0.682 | 3.070 | 0.163 | 1.629 | 3.440 | 0.303 | 3.030 |
| FS (MPa) | 10 | 7.000 | 0.037 | 0.370 | 8.500 | 0.259 | 2.593 | 9.500 | 0.407 | 4.074 |
| UPV | 10 | 4.220 | -0.012 | -0.117 | 4.500 | 0.054 | 0.539 | 4.550 | 0.066 | 0.656 |
| Freeze-thaw process up to 120 cycles | 10 | 59.280 | 0.056 | 0.557 | 63.820 | 0.137 | 1.366 | 66.220 | 0.179 | 1.793 |
| RCPT | 10 | 2759.000 | 0.048 | 0.483 | 3200.000 | 0.216 | 2.158 | 3540.000 | 0.345 | 3.450 |
| | | | | 3.029 | | | 10.483 | | | 15.873 |
| Benefit | | 3.029 | | | 10.483 | | | 15.873 | | |
| Cost INR ($) | | 5084 | | | 5340 | | | 5597 | | |
| BCR × 100 | | 0.060 | | | 0.063 | | | 0.026 | | |

**Table 20**. BCRs of NT concrete.

(0.063), indicating that the performance gains were sufficiently counterbalanced by the added material cost. On the other hand, the 1.5% NT mixture had the lowest ratio (0.026), indicating that the cost added was way more than the gains received. Since the prices of cement, coarse aggregate, fine aggregate, and superplasticizer were the same throughout all mixtures, the difference in benefit-cost ratio is largely due to the price of the NT. These findings point to an especially important issue concerning the practical use of NT in concrete: its performance-improving attributes are rather NT's cost, which limits its practicality, especially to low-cost use cases. Therefore, lower dosages of NT might be a more practical approach to use NT in concrete where performance and economic practicality are of high importance.

## Real world application (Scenario Setup)

This assessment analyzes the use of NT enhanced concrete economically for a marine infrastructural project in India, wherein the durability issue caused by the chloride induced corrosion is critical. The target conventional concrete is designed at a characteristic compressive strength of 50.66 MPa, costing ₹ 4827 per cubic meter. The nano-modified concrete, which incorporates 1.0% NT, has a compressive strength of 61.8 MPa and results in the unit material cost rising to ₹ 5340 per cubic meter. The nano-modified concrete is priced at ₹ 140 per kg and the nano-additive concrete's incremental cost is ₹ 513 per cubic meter. The key focus in this assessment is the increase in the service life, which is value-adding. Major repairs are expected to be needed on the conventional

| Property | 0.5NT (Delta cost = 256.5) | | | 1.0NT (Delta cost = 513) | | | 1.5NT (Delta cost = 769.5) | | |
|---|---|---|---|---|---|---|---|---|---|
| | B Eq. 7 | B Eq. 9 | BCR Eq. 10 | B Eq. 7 | B Eq. 9 | BCR Eq. 10 | B Eq. 7 | B Eq. 9 | BCR Eq. 10 |
| CS (MPa) | 0.105 | 254.404 | 0.992 | 0.220 | 530.722 | 1.035 | 0.287 | 692.702 | 0.900 |
| STS (MPa) | 0.068 | 164.557 | 0.642 | 0.163 | 393.108 | 0.766 | 0.303 | 731.364 | 0.950 |
| FS (MPa) | 0.037 | 89.389 | 0.348 | 0.259 | 625.722 | 1.220 | 0.407 | 983.278 | 1.278 |
| UPV | -0.012 | -28.261 | -0.110 | 0.054 | 130.001 | 0.253 | 0.066 | 158.262 | 0.206 |
| RCPT | 0.048 | 116.457 | 0.454 | 0.216 | 520.847 | 1.015 | 0.345 | 832.621 | 1.082 |
| | | | 0.454 | | | 1.015 | | | 0.950 |

**Table 21**. Simple BCR for strength gain of NT concrete.

concrete after 25 years due to chloride penetration, while the NT-concrete is expected to postpone this by 10 years; thus, major repairs would be first required at the 35-year mark. This assessment assumes that the repair cost for the pier deck is ₹ 1,68,00,000, which is 200,000 USD at an exchange rate of $1 = ₹ 84. Within the context of anticipating repair expenditures on the NPV construction, the net present value of future repair savings is estimated considering a discount rate of 5% over the 50-year analysis horizon. The analysis assumes a repair cost of ₹1,68,00,000 (equivalent to $200,000 at an exchange rate of 1 USD = 84 ₹) for the pier deck. A discount rate of 5% is applied over a 50-year analysis period to compute the net present value (NPV) of future repair savings, thereby contextualizing the higher initial investment within a long-term lifecycle cost framework. This scenario provides a realistic basis for assessing the value proposition of nanotechnology in construction within the Indian market.

*Simple BCR for strength gain*

To assess the improvement along with cost, the third metric should be Monetized Benefit (see Eq. 9). The benefit-cost ratio analysis, when myopically centered on CS enhancement, gives a value of roughly 1.015 for the nano-titanium modified concrete, as presented in Table 18. This indicates a slight economic benefit, in terms of an additional 22% strength gain, which just surpasses the extra cost incurred in the nanomaterial (see Table 21). This outcome, however, must be viewed with a level of skepticism. A BCR that is close to but less than 1.0 shows a fragile economic case where strength is the only consideration (see Eq. 10)[70,71]; minor changes in the cost of the materials or performance variability could easily erase this slim advantage. This highlights the limitation of evaluating new materials using a singular mechanical lens.

$$\text{Monetized Benefit (B)} = \text{b} \times \alpha \times \text{Cost} \tag{9}$$

Assume a value of $\alpha$ = 0.5₹, means each 1% strength increase is valued at 0.5% of the concrete cost.

$$\text{BCR} = \frac{\text{B}}{\Delta\, Cost_{total}} \tag{10}$$

*Lifecycle cost (LCC) analysis*

While the simplified engineering benefit–cost ratio focused only on strength provides a certain viewpoint, a more thorough assessment should consider the added economic value of enhanced durability over time. LCC analysis provides this perspective[69,70], as it measures the value of maintenance deferred, as well as the enormous cost savings over the operational life of the structure, attributable to the enhanced performance of NT of concrete. The analysis presented in Eqs. 11–13 shows that deferring the major repair from year 25 to year 35 results in a net present value of avoided costs of ₹19.2 lakh, which is significant. Also, as a comparison, the nano concrete variant requires an additional initial material investment of ₹5.1 lakh. In this scenario, the nano concrete variant provides a net lifecycle saving of ₹14.1 lakh. The results support a capital expenditure on the structure on account of durability and the shed expenditure, while the structure determines operational efficiency, the shed is therefore a rational investment. The assessment, therefore, shifts from a simplistic expenditure to value accretion over time. This underscores a critical principle in sustainable infrastructure: funding for technology that adds value by enhancing durability is not a cost, but a financial instrument that reduces obligation and risk for the duration of the asset's life cycle. The results of the CBA suggest that a positive NPV, together with a BCR greater than one, offers a compelling economic rationale for the expenditure[69,73]. These indicators reinforce the notion that the benefits to be gained are greater than the expenditure and recurring disbursements, which, from a financial perspective, significantly justify the solvency and strategic imperative of the project[73,74].

$$\text{NPV}_{\text{conventional concrete}} = \frac{Repair\ cost}{(1+0.05)^{T}} \tag{11}$$

$$\text{NPV}_{\text{conventional concrete}} = \frac{1,68,00,000}{(1+0.05)^{25}} = ₹49,61,836$$

$$\text{NPV}_{\text{NT concrete}} = \frac{1,68,00,000}{(1+0.05)^{35}} = ₹30,39,258$$

$$Avoided\ Repair\ Cost\ (B_{\text{delay}}) = \text{NPV}_{\text{conventional concrete}} - \text{NPV}_{\text{NT concrete}} \quad (12)$$

$$B_{\text{delay}} = ₹49,61,836 - ₹30,39,258 = ₹19,22,578$$

$$\Delta_{\text{Initial Cost for 1000 m}^3} = (₹5340 - ₹4827) \times 1000 = ₹5,13,000$$

$$Net_{\text{savings}} = B_{\text{delay}} - \Delta_{\text{Initial Cost for 1000 m}^3} \quad (13)$$

$$Net_{\text{savings}} = ₹19,22,578 - ₹5,13,000 = ₹14,09,578$$

*Break-even analysis*

The break-even analysis identifies the maximum allowable cost for NT where the lifecycle savings from delayed repair just offset the initial investment. The formula used is (Eq. 14):

$$\text{C}_{\text{nt, BE}} = \frac{B_{\text{delay}}}{total\ NT\ for\ 1000\ \text{m}^2\ of\ concrete} \quad (14)$$

$$\text{C}_{\text{nt,BE}} = \frac{19,22,578}{3800} = ₹505.94/\text{kg}$$

Based on the break-even analysis, material scientists and other stakeholders were able to study the techomics of using titanium nano-dioxide in concrete and ascertain the benefits of using the material throughout the lifecycle. The analysis estimates that the benefits of not spending money on major repairs for a decade alone can justify spending a total cost of upto ₹506 on a nanomaterial. This is worth contrast to the current price of ₹140, showing a large margin that can sustain conservative estimates. Provided the cost of NT does not exceed ₹506, the NT-concrete becomes economically viable for this construction project. This large buffer suggests not only that the NT technology is likely to remain economically viable given current conditions, but also that there is a large buffer in case of cost inflation in the future. It shifts the question away from, 'is nano titanium dioxide economically viable?' to 'how much economic loss can the project sustain and still be viable?' This also allows investors to rest assured that spending on the material enhancement technology is economically sensible in the future.

## Conclusion

Based on an extensive experimental investigation into the mechanical, petrographic, microstructural, and durability properties of NT-incorporated concrete along with economic analysis, the following conclusions are drawn:

(1) The incorporation of NT significantly enhances the CS of concrete matrix, producing a high-strength nanocomposite. A conventional M40-grade mix transforms into high-strength concrete with NT, achieving a peak CS of 75.25 MPa at 180 days with 1.5% NT incorporation, compared to 58.80 MPa for normal mix concrete.
(2) At 28 days, NT incorporation at 0.5%, 1%, and 1.5% increased CS by 10.54%, 21.98%, and 28.70%, respectively, compared to normal concrete. A similar trend was observed for STS and FS, with improvements of 30.30% and 40.74%, respectively, at 1.5% NT dosage. However, workability decreased as NT content increased.
(3) NT effectively improves fracture properties by controlling matrix cracks at the nano-scale, as confirmed through SEM analysis. The material also exhibits a crack-bridging mechanism, leading to a denser and more resilient concrete structure.
(4) Petrographic studies confirm the absence of micropores in both cement paste and the concrete matrix, indicating an improved microstructural integrity due to NT incorporation. Additionally, SEM analysis highlights the densification effect of NT, contributing to enhanced durability.
(5) NT-modified concrete demonstrated superior resistance to aggressive environments. When exposed to 4% HCl for 90 days, CS improved by 5.93%, 17.70%, and 28.72% with 0.5%, 1%, and 1.5% NT, respectively. Similarly, exposure to 4% $H_2SO_4$ resulted in strength gains of 15.35%, 30.28%, and 42.94%.
(6) NT contributed to improved freeze-thaw resistance by reducing pore space, limiting water penetration, and minimizing freeze-induced deterioration. Additionally, its fine particle size and pore-filling capacity significantly reduced chloride ion permeability, preventing carbonation and enhancing resistance to chloride ingress.
(7) Under elevated temperatures, NT-incorporated concrete exhibited a notable strength increase. At 300 °C, a maximum strength gain of 35.89% was recorded at 1.5% NT dosage, attributed to additional cement hydration and the pozzolanic reactivity of NT. However, at 600 °C, CS declined beyond a 0.5% NT dosage due to thermal degradation.
(8) The tangent modulus of elasticity improved with increasing NT content, reaching a maximum of 8.25 GPa at 1.5% NT incorporation, further reinforcing NT's role in enhancing concrete stiffness and overall mechanical performance.
(9) The benefit-cost analysis demonstrates that the economic viability of NT in concrete is highly dosage-dependent. The 1.0% NT mixture represents the optimal compromise between performance enhancement and cost efficiency under current market conditions.

(10) The data on life-cycle costs illustrates that NT-concrete's economic value is considerable because net savings are over ₹14 lakh even with increasing initial expenses, because of the ample service life extension NT-concrete provides. The current market conditions indicate that the economic viability of the technology is excellent, given that the market price would have to be approximately ₹506 per kilogram to break even on the NT costs, which is far below current market prices. These results corroborate that the carefully planned purchase of NT-concrete is a reasonable investment from both a technoeconomic and practical standpoint.

This study underscores the potential of NT as a transformative nanomaterial in concrete technology, improving strength, durability, and resistance to aggressive environments while optimizing microstructural properties. It should be noted that the specific crystalline phase (anatase vs. rutile) of the nano-titanium dioxide used in this study was not characterized via XRD. Investigating the influence of phase composition on the resulting concrete properties presents a valuable direction for future research.

## Data availability

The datasets used and/or analysed during the current study available from the corresponding author on reasonable request.

Received: 19 July 2025; Accepted: 3 October 2025
Published online: 10 November 2025

## References

1. Karimi Sahnesarayi, M., Sarpoolaky, H. & Rastegari, S. Effect of heat treatment temperature on the performance of nano-TiO2 coating in protecting 316L stainless steel against corrosion under UV illumination and dark conditions. *Surf. Coat. Technol.* **258**, 861–870 (2014).
2. Dey, T. UV-reflecting sintered nano-$TiO_2$ thin film on glass for anti-bird strike application. *Surf. Eng.* **37**, 688–694 (2021).
3. Dudczig, S., Veres, D., Aneziris, C. G., Skiera, E. & Steinbrech, R. W. Nano- and micrometre additions of $SiO_2$, $ZrO_2$ and $TiO_2$ in fine grained alumina refractory ceramics for improved thermal shock performance. *Ceram. Int.* **38**, 2011–2019 (2012).
4. Ferrari, A., Pini, M., Neri, P. & Bondioli, F. Nano-$TiO_2$ coatings for limestone: which sustainability for cultural heritage? *Coatings* **5**, 232–245 (2015).
5. Rawat, G., Gandhi, S. & Murthy, Y. I. Strength and rheological aspects of concrete containing nano-titanium dioxide. *Asian J. Civil Eng.* **23**, 1197–1208 (2022).
6. Shchelokova, E. A., Tyukavkina, V. V., Tsyryatyeva, A. V. & Kasikov, A. G. Synthesis and characterization of SiO2-TiO2 nanoparticles and their effect on the strength of self-cleaning cement composites. *Constr. Build. Mater.* **283**, 122769 (2021).
7. Seddik Meddah, M. Durability performance and engineering properties of shale and volcanic ashes concretes. *Constr. Build. Mater.* **79**, 73–82 (2015).
8. Zhang, R., Cheng, X., Hou, P. & Ye, Z. Influences of nano-TiO2 on the properties of cement-based materials: Hydration and drying shrinkage. *Constr. Build. Mater.* **81**, 35–41 (2015).
9. Patil, A. et al. Performance analysis of self-compacting concrete with use of artificial aggregate and partial replacement of cement by fly Ash. *Buildings* **14**, 143 (2024).
10. Ige, O. E., Olanrewaju, O. A., Duffy, K. J. & Obiora, C. A review of the effectiveness of life cycle assessment for gauging environmental impacts from cement production. *J. Clean. Prod.* **324**, 129213 (2021).
11. Han, Y. et al. Optimization of the life cycle environmental impact of shell powder and slag concrete using response surface methodology. *Process Saf. Environ. Prot.* **194**, 272–288 (2025).
12. Schneider, M., Hoenig, V., Ruppert, J. & Rickert, J. The cement plant of tomorrow. *Cem. Concr Res.* **173**, 107290 (2023).
13. Deng, Z. et al. Advantages and disadvantages of PVA-fibre-reinforced slag- and fly ash-blended geopolymer composites: engineering properties and microstructure. *Constr. Build. Mater.* **349**, 128690 (2022).
14. Deng, Z. & Deng, Z. Short-term improvement of ductile geopolymer composites exposed to magnesium sulfate: Mechanical properties, sorptivity, and mechanisms. *Constr. Build. Mater.* **408**, 133648 (2023).
15. Deng, Z., Zhang, S. & Deng, Z. PVA fiber-reinforced geopolymer mortar made with hybrid recycled aggregates: Toward thermal insulation, lightweight and improved durability. *J. Clean. Prod.* **426**, 139200 (2023).
16. Deng, Z. Influence of recycled rubber and glass aggregates on magnesium sulfate resistance of geopolymers: Physio-mechanical properties and mechanisms. *Constr. Build. Mater.* **438**, 137134 (2024).
17. Deng, Z., Lin, J. & Li, N. A review on recycling seashells as aggregates and binders for mortar and concrete in china: Production, engineering properties and new applications. *Sustainable Mater. Technol.* **43**, e01242 (2025).
18. Paruthi, S. et al. A comprehensive review of nano materials in geopolymer concrete: Impact on properties and performance. *Dev. Built Environ.* **16**, 100287 (2023).
19. Jenima, J. et al. A comprehensive review of titanium dioxide nanoparticles in cementitious composites. *Heliyon* **10**, e39238 (2024).
20. Çelik, F., Yıldız, O. & Batur Çolak, A. An experimental investigation on workability and bleeding behaviors of cement pastes doped with nano titanium oxide (n-$TiO_2$) nanoparticles and fly ash. *Fluid Dyn. Mater. Process.* **19**, 135–158 (2023).
21. Joshaghani, A., Balapour, M., Mashhadian, M. & Ozbakkaloglu, T. Effects of nano-TiO2, nano-Al2O3, and nano-Fe2O3 on rheology, mechanical and durability properties of self-consolidating concrete (SCC): An experimental study. *Constr. Build. Mater.* **245**, 118444 (2020).
22. Li, S. et al. The performance and functionalization of modified cementitious materials via nano titanium-dioxide: A review. *Case Stud. Constr. Mater.* **19**, e02414 (2023).
23. Meng, T., Yu, Y., Qian, X., Zhan, S. & Qian, K. Effect of nano-$TiO_2$ on the mechanical properties of cement mortar. *Constr. Build. Mater.* **29**, 241–245 (2012).
24. Sun, Y., Zhang, P., Guo, W., Bao, J. & Qu, C. Effect of Nano-$CaCO_3$ on the mechanical properties and durability of concrete incorporating fly ash. *Adv. Mater. Sci. Engi.* (2020).
25. Gopala, K., Sastry, K. V. S., Sahitya, P. & Ravitheja, A. Influence of nano $TiO_2$ on strength and durability properties of geopolymer concrete. *Mater. Today Proc.* **45**, 1017–1025 (2021).
26. Nazari, A. & Riahi, S. The effects of $TiO_2$ nanoparticles on physical, thermal and mechanical properties of concrete using ground granulated blast furnace slag as binder. *Mater. Sci. Eng.: A* **528**, 2085–2092 (2011).
27. Ren, J., Lai, Y. & Gao, J. Exploring the influence of $SiO_2$ and $TiO_2$ nanoparticles on the mechanical properties of concrete. *Constr. Build. Mater.* **175**, 277–285 (2018).
28. Chinthakunta, R., Ravella, D. P., Rama Chand, S., Janardhan Yadav, M. & M. & Performance evaluation of self-compacting concrete containing fly ash, silica fume and nano titanium oxide. *Mater. Today Proc.* **43**, 2348–2354 (2021).

29. Farzadnia, N., Ali, A., Demirboga, A. A., Anwar, M. P. & R. & Characterization of high strength mortars with nano titania at elevated temperatures. *Constr. Build. Mater.* **43**, 469–479 (2013).
30. Luo, Z., Yang, L. & Liu, J. Embodied carbon emissions of office building: A case study of china's 78 office buildings. *Build. Environ.* **95**, 365–371 (2016).
31. IS: 8112 – 2013. Ordinary Portland Cement, 43 Grade - Specification. (2013).
32. IS 2386 (Part I). Methods of Test for Aggregates for Concrete Part I Particle Size and Shape. (2016).
33. IS: 383. Coarse and Fine Aggregate for Concrete-Specification. (2016).
34. IS: 456. Plain and Reinforced Concrete - Code of Practice. (2000).
35. Tobaldi, D. M., Pullar, R. C., Seabra, M. P. & Labrincha, J. A. Fully quantitative X-ray characterisation of Evonik aeroxide TiO2 P25®. *Mater. Lett.* **122**, 345–347 (2014).
36. Manuputty, M. Y., Lindberg, C. S., Botero, M. L., Akroyd, J. & Kraft, M. Detailed characterisation of $TiO_2$ nano-aggregate morphology using TEM image analysis. *J. Aerosol Sci.* **133**, 96–112 (2019).
37. IS: 1199. *Fresh Concrete—Methods of Sampling, Testing and Analysis*. (2018).
38. IS: 4031 (Part 6). Determination of Compressive Strength of Hydraulic Cement Other than Masonry Cement. (1988).
39. IS: 516. Indian Standard Methods of Tests for Strength of Concrete. (2021).
40. IS: 5816. *Method of Test for Splitting Tensile Strength of Concrete*. (2004).
41. Paruthi, S., Rahman, I., Khan, A. H., Sharma, N. & Alyaseen, A. Strength, durability, and economic analysis of GGBS-based geopolymer concrete with silica fume under harsh conditions. *Sci. Rep.* **14**, 31572 (2024).
42. IS: 13311(2). Non-Destructive Testing of Concrete - Method of Test - Part II Rebound Hammer. (1992).
43. IS 13311 Part 1. 1992 Method of Non-Destructive Testing of Concret: I. Ultrasonic Pulse Velocity. (1992).
44. ASTM C666/C666M. Standard test method for resistance of concrete to rapid freezing and thawing. *ASTM Int. West. Conshohocken* 1–6 (2003).
45. AASHTO, T. *Standard Method of Test for Surface Resistivity Indication of Concrete's Ability to Resist Chloride Ion Penetration.*. (2011).
46. AASHTO T277. Standard Method of Test for Rapid Determination of the Chloride Permeability of Concrete. (1993).
47. ASTM C1202. Standard Test Method for Electrical Indication of Concrete's Ability to Resist Chloride Ion Penetrationk. (2022).
48. IS 3085. Method of Test for Permeability of Cement Mortar and Concrete. (1965).
49. Tanimola, J. O. & Efe, S. Recent advances in nano-modified concrete: enhancing durability, strength, and sustainability through nano silica (nS) and nano titanium (nT) incorporation. *Appl. Eng. Sci.* **19**, 100189 (2024).
50. Mousavi, M. A. et al. Strength optimization of cementitious composites reinforced by carbon nanotubes and titania nanoparticles. *Constr. Build. Mater.* **303**, 124510 (2021).
51. Nazari, A., Riahi, S., Riahi, S., Shamekhi, S. F. & Khademno, A. Influence of $Al_2O_3$ nanoparticles on the compressive strength and workability of blended concrete. *J. Am. Sci.* **6**, 6–9 (2010).
52. Atiq Orakzai, M. Hybrid effect of nano-alumina and nano-titanium dioxide on mechanical properties of concrete. *Case Stud. Constr. Mater.* **14**, e00483 (2021).
53. Jeng, Y. R., Tsai, P. C. & Chiang, S. H. Effects of grain size and orientation on mechanical and tribological characterizations of nanocrystalline nickel films. *Wear* **303**, 262–268 (2013).
54. Rahman, I. et al. Improvements in the engineering properties of cementitious composites using nano-sized cement and nano-sized additives. *Materials* **15**, 8066 (2022).
55. Baikerikar, A. V. et al. Synergistic effects of nano titanium dioxide and waste glass powder on the mechanical and durability properties of concrete. *Sci. Rep.* **14**, 27573 (2024).
56. Ghanim, A. A. J., Amin, M., Zeyad, A. M., Tayeh, B. A. & Agwa, I. S. Effect of modified nano-titanium and fly ash on ultra-high-performance concrete properties. *Struct. Concr.* **24**, 6815–6832 (2023).
57. Sellevold, E. J. & Bjøntegaard, Ø. Coefficient of thermal expansion of cement paste and concrete: mechanisms of moisture interaction. *Mater. Struct.* **39**, 809–815 (2006).
58. Wan, X., Su, C. & Li, L. Effects of nano silica on carbonation resistance of concrete. *MATEC Web Conferences*. **275**, 02001 (2019).
59. Snehal, K., Das, B. B. & Barbhuiya, S. Synergistic effect of nano silica on carbonation resistance of multi-blended cementitious mortar. *Cem. Concr Compos.* **141**, 105125 (2023).
60. Guler, S., Türkmenoğlu, Z. F. & Ashour, A. Performance of single and hybrid nanoparticles added concrete at ambient and elevated temperatures. *Constr. Build. Mater.* **250**, 118847 (2020).
61. Wu, L., Lu, Z., Zhuang, C., Chen, Y. & Hu, R. Mechanical properties of nano $SiO_2$ and carbon fiber reinforced concrete after exposure to high temperatures. *Materials* **12**, 3773 (2019).
62. Brzozowski, P. et al. Effect of Nano-$SiO_2$ on the microstructure and mechanical properties of concrete under high temperature conditions. *Materials* **15**, 166 (2021).
63. Nasehi Ghashouieh, M., Malekinejad, M. & Amiri, M. Microstructural analysis of the effect of using nano-silica on the mechanical properties of cement–sand mortar under the effect of heat. *Int. J. Concr Struct. Mater.* **18**, 74 (2024).
64. Rawat, G., Gandhi, S. & Murthy, Y. I. Durability aspects of concrete containing Nano- titanium dioxide. *ACI Mater. J.* **120** (2023).
65. Mohammadi, M., Hesaraki, S. & Hafezi-Ardakani, M. Investigation of biocompatible nanosized materials for development of strong calcium phosphate bone cement: Comparison of nano-titania, nano-silicon carbide and amorphous nano-silica. *Ceram. Int.* **40**, 8377–8387 (2014).
66. Abdullah, G. M. S. et al. Effect of titanium dioxide as nanomaterials on mechanical and durability properties of rubberised concrete by applying RSM modelling and optimizations. *Front Mater* **11** (2024).
67. Bautista-Gutierrez, K. P., Herrera-May, A. L., Santamaría-López, J. M., Honorato-Moreno, A. & Zamora-Castro, S. A. Recent progress in nanomaterials for modern concrete infrastructure: advantages and challenges. *Materials* **12**, 3548 (2019).
68. Ebrahim, A. et al. Synergistic effects of combined multi-walled carbon nanotubes and glass fibers on concrete: experimental and economic analysis. *Fullerenes Nanotubes Carbon Nanostruct.* **33**, 657–673 (2025).
69. Li, J., Sha, A., Wang, Z., Song, R. & Cao, Y. Investigation of the self-healing, road performance and cost–benefit effects of an iron tailing/asphalt mixture in pavement. *Constr. Build. Mater.* **422**, 135788 (2024).
70. Kabakian, V. & McManus, M. From private to social cost-benefit analysis: life cycle environmental impact cost internalization in cement production fuel switching. *Environ. Dev. Sustain.* **26**, 25527–25548 (2023).
71. Alzein, R. et al. Polypropylene waste plastic fiber morphology as an influencing factor on the performance and durability of concrete: Experimental investigation, soft-computing modeling, and economic analysis. *Constr. Build. Mater.* **438**, 137244 (2024).
72. Alyaseen, A. et al. Influence of silica fume and *Bacillus subtilis* combination on concrete made with recycled concrete aggregate: Experimental investigation, economic analysis, and machine learning modeling. *Case Stud. Constr. Mater.* **19**, e02638 (2023).
73. Hsu, E. Cost-benefit analysis for recycling of agricultural wastes in Taiwan. *Waste Manag.* **120**, 424–432 (2021).
74. Liu, G., Hua, J., Wang, N., Deng, W. & Xue, X. Material Alternatives for Concrete Structures on Remote Islands: Based on Life-Cycle-Cost Analysis. *Adv. Civ. Eng.* (2022).


## Acknowledgements

AcknowledgmentThe authors gratefully acknowledge the funding of the Deanship of Graduate Studies and Scientific Research, Jazan University, Saudi Arabia, through project number: (JU-202505352-DGSSR-ORA-2025).

The support from all participating institutions—Jamia Millia Islamia (India), K.R. Mangalam University (India), Delhi Technological University (India), Aligarh Muslim University (India), Jazan University (Saudi Arabia), Malla Reddy Engineering College (India), and Al-Furat University (Syria)—is also gratefully acknowledged.

## Author contributions

I.R. and S.P.: Conceptualization, Data curation, Investigation, Methodology, Validation, Visualization, Writing—original draft, Writing—review & editing. I.R., N.D., and M.A.: Supervision, Validation, Visualization. N.D., M.A., and C.V.S. R.P.: Writing—review & editing, Validation. A.H.K., A.A., and M.A.H.: Writing—review & editing, Validation, Visualization, and Funding.

## Funding

The authors gratefully acknowledge the funding of the Deanship of Graduate Studies and Scientific Research, Jazan University, Saudi Arabia, through project number: (JU-202505352-DGSSR-ORA-2025).

## Declarations

## Competing interests

The authors declare no competing interests.

## Additional information

**Supplementary Information** The online version contains supplementary material available at https://doi.org/10.1038/s41598-025-22974-4.

**Correspondence** and requests for materials should be addressed to A.H.K. or A.A.